SELECTED VALENCE ELECTRON MODEL FOR HALOGEN-SUBSTITUTED PLANAR PI-MOIETY MOLECULES AND SMALL SIGMA-BONDED SYSTEMS

By

DARREL GENE HOPPER

Bachelor of Science

Oklahoma State University

Stillwater, Oklahoma

1966

Submitted to the Faculty of the Graduate College
of the Oklahoma State University
in partial fulfillment of the requirements
for the Degree of
DOCTOR OF PHILOSOPHY
July, 1971

SELECTED VALENCE ELECTRON MODEL FOR HALOGEN-SUBSTITUTED PLANAR PI-MOIETY MOLECULES AND SMALL SIGMA-BONDED SYSTEMS

Thesis Approved:

Leonil M. Raff
Thesis Adviser

Herbert A. Pohl

J. Paul Devlin

Neil Purdie

Clarence M. Cunningham

A. Durham
Dean of the Graduate College

ACKNOWLEDGEMENTS

I thank Dr. Lionel M. Raff, my advisor, for his excellent teaching, advise, and patient guidance throughout the period of this study. Dr. Herbert A. Pohl, co-advisor for this thesis, I thank for initial suggestions on the problem, for his advise on several points of procedure, and for his always instructive conversations. I am grateful to the other members of my committee--Drs. Clarence M. Cunningham, J. Paul Devlin, Robert D. Freeman, and Neil Purdie--for serving on my behalf. I thank Dr. Timothy M. Wilson for a very helpful discussion of the Hartree-Fock-Slater potential.

For personal and research support I am indebted to the Department of Health, Education, and Welfare for a National Defense Education Act Title IV Fellowship, to the American Chemical Society for a Petroleum Research Foundation Fellowship, and to the Oklahoma State University Research Foundation. Dr. Otis T. Dermer, Chairman of the Chemistry Department, has my gratitude for making a number of part-time Graduate Teaching Assistantships available to me. In addition, the services rendered by the Oklahoma State University Computer Center are strongly appreciated.

I commend Janet Sallee for her competent typing of this thesis.

My wife, Chahira Metwally, has contributed to this thesis both directly and indirectly. She has done an excellent job of preparing the illustrations. But more importantly, she has provided me with creative motivation by helping life to ring clear to me culturally and emotionally as well as professionally and logically.

TABLE OF CONTENTS

TABLE OF CONTENTS (Continued)

LIST OF TABLES

LIST OF TABLES (Continued)

LIST OF FIGURES

. . .

LIST OF FIGURES (Continued)

CHAPTER I

INTRODUCTION

The theoretical prediction of molecular properties is a subject central in chemistry. Research results in this century demonstrate that quantum mechanics is a valid theory with which to treat a molecule as a collection of electrons and nucleus-like particles. While much is known about the ways and means of application of quantum theory molecules and about the levels of confidence and practical limitations of many procedures[1], a greater amount is yet to be discovered.

The Case for Semiempirical Models

The application of a quantum mechanics to a molecule involves severe mathematical difficulties. As Dirac[2] realized in 1929, but for these difficulties, chemistry is a mathematical science. However, the outlook is more optimistic for computational chemistry today than it was forty years ago. The continuing evolution of even more efficient approximate methods and computational machinery is now beginning to open the way to an extensive exploration of the full capabilities of quantum chemistry. For example, the main problem with the Hartree-Fock LCAO-MO-SCF approach[1], itself a breakthrough as an approximate procedure, has been the evaluation of three and four center integrals[3]. Over the last decade computers and special techniques have dramatically reduced this integral problem. Thus, neglecting electron correlation, a molecu-

lar system of small to intermediate size (about 20 atoms) can now be fairly well treated by the HF-LCAO-MO-SCF ab initio approximate quantum mechanical method. The extensive computations by Clementi[4,5] on the reaction

$$NH_3 + HCl \rightarrow NH_4Cl$$

exemplifies the point. But computations are impractically expensive for big molecules or for the large number of nuclear configurations required for the computation of an equilibrium molecular geometry or a reaction potential surface. Therefore, there is a cost-return balance in the favor of quantum methods yet more approximate than the ab initio ones, semiempirical in particular. In semiempirical molecular theories the integral evaluation problem is solved by systematically approximating the integrals with experimental information about atoms or molecules or both. In addition, such theories customarily restrict explicit consideration to valence electrons.

Quantum chemistry is only now beginning to become an exact science. As the present transition from empirical to mathematical chemistry proceeds, semiempirical methods can be profitably used in exploring the application of quantum theory to molecules.

Pi and All-Valence Methods

Current semiempirical methods may be classified into two groups: pi-valence electron and all-valence electron. The first group (e.g. Hückel[1], Pariser-Parr-Pople[6,7]) address the problem of describing those molecular properties determined by the pi-electron system of a planar molecule. The inner-shell and in-plane sigma-bonding valence electrons

are implicitly considered through their influence on the experimental data used for the pi-electrons and through their assumed exact cancellation of a unit of nuclear charge in the pi-electron potential. The second group (e.g. extended Hückel[8], CNDO[9-11], INDO[12], NDDO[9], KINDO[13], EMZDO[14], PNDO[15], MINDO[16,17]) take into explicit consideration all of the valence electrons but treat the inner-shell atomic electrons implicitly, as do the pi methods.

The pi-electron models are capable of predicting the pi-electron determined parts of molecular spectra, dipole moments, and relative reactivities and stabilities by computations at the experimental molecular geometry. The all-valence methods can predict, in addition to the equilibrium properties, the equilibrium geometry itself if properly parameterized and calibrated to a set of experimental information.

Fischer-Hjalmer's[18] comparative study of the pi-electron system of the aniline molecule by Hückel, Pariser-Parr-Pople, and ab initio methods is a representative example of a pi model. The Pariser-Parr-Pople method was found to best predict the molecular ionization potential and electron affinity, the pi-component of the dipole moment, and a reasonable set of atomic charges. The Pariser-Parr-Pople method was also found to be much less sensitive to the input data than the more approximate Hückel method. The model developed in this thesis is similar in many respects to the Pariser-Parr-Pople method.

A recent example of an all-valence model is provided by the paper of Dewar and Haselbach[17] on their MINDO/2 scheme. MINDO/2 is a modified version of the intermediate neglect of differential overlap model (INDO) of Pople, Beveridge, and Dobosh[12]. The principle modifications are that (a) experiment is taken as a reference instead of ab initio Hartree-Fock

results and (b) two parameters for each of several different atom pairs are used to calibrate the model. The parameters are determined by a least squares fit to the experimental heats of formation of an assumed set of standard molecules and to the equilibrium length of one bond in each of them. The two parameters per atom pair are a parameter similar to that of Wolfsberg and Helmholz[19] and an exponential constant in the core repulsion expression employed. Like INDO, MINDO/2 neglects all integrals involving the product of atomic orbitals on different atoms and equates the remaining two-center electron repulsion and core attraction integrals by evaluating them with identical approximation expressions. One-center integrals are given values systematically determined from atomic spectral data. The results for hydrocarbons from methane to toluene[17] and for oxygen and nitrogen containing molecules from water to aniline[20] are good except for triple bonds. Bond lengths, heats of formation, and force constants are simultaneously predicted quantitatively.

Dewar and Haselbach's[17] work illustrates a way by which semiempirical methods can be made accurate; calibration of atom pair parameters to the experimental molecular quantities of interest. Such a procedure must be employed if the numerous approximations of a semiempirical method are to be properly compensated.

Selected-Valence Methods

Considering the successes of both the pi- and the all-valence electron approaches, the question of how many electrons need to be explicitly considered for a given molecular system arises. That is, given the molecular quantities one wishes to predict, how much input information is required?

Pohl, Rein, and Appel[21], Harris and Pohl[22], and Pohl and Raff[23] have shown that many diatomics may be described by explicit consideration of only the bonding electron pair. A four-electron model of the three-atom hydrogen bond system X-H---Y has been found by Mickish and Pohl[24] and Cantril and Pohl[25] to yield reasonable results for the hydrogen position, force constants, and bond energies. Rein and Harris[26] find that the hydrogen bond of the guanine-cytosine base pair can be qualitatively described by a consideration of only the four-hydrogen bonding electrons together with the twenty-four pi-electrons.

Yet another example of a successful model that takes account of only a few valence electrons is the four-electron H_2I_2 potential surface computation reported recently by Raff, Stivers, Porter, Thompson and Sims[27]. They employ a non-ionic valence-bond wave functional form together with simplifying integral approximations introduced by London[28,29] Eyring and Polanyi[30], Sato[31], and Cashion and Herschbach[32]. Experimental molecular data for the diatomics H_2, I_2, and HI are used except for the triplet energy curves of HI and I_2, which they compute semiempirically. A parameter in the approximation expression for the one-center core-attraction integral on iodine is used to adjust the activation energy of the computed surface to the experimental value[33]. The regular planar trapezoidal saddle point is found to be the most stable, followed by the symmetric linear.

The Problem

The clear implication of the works described above is that there is the definite possibility of systematically describing a number of properties of molecules with a semiempirical model that treats a subset of the

valence electrons. While this possibility is contrary to the trend of the past few years toward all-valence models, its exploration can help to determine how much and what kind of experimental information is required for molecular property predictions. If such an intermediate model can reasonably well describe those molecule properties it considers, then it could be calibrated to a set of experimental molecular data and used to accurately predict those properties. A calibrated model could also be used to compute reaction potential surfaces. One approach could be the use of computed results for a large number of reaction system configurations to determine the parameters of an appropriate surface potential functional form. An intermediate model would have the advantage of being less costly to use than an all-valence model.

To study the above possibility, this thesis defines a selected valence electron model (SVEM) and examines its application to substituded planar pi-moiety molecules and radicals and to H_2I_2 saddle point configurations. The model here examined singles out for explicit consideration the pi electrons and/or some selected sigma electrons. Various integral approximation expressions commonly employed in semiempirical theories are tried and used without inserting any calibration parameters. The HF-SCF-LCAO-MO approximate wave function formalism is employed in both restricted (all spatial MO's required to appear in two spin MO's) and unrestricted form. The model is developed in Chapter II.

The pi-moieties considered are ethene, ethyne, and benzene at their experimental geometries in the substituted molecules. The halogens are taken as substituents. In Chapter III the singly substituted series RF, RCl, RBr, RI is considered for each pi-moiety. For each pi molecule the equilibrium C-X distances, bond energies, and stretching frequencies are

computed at the known bond angles. The results are compared to experiment.

In Chapter IV the ability of the model to describe multiply substituted molecules and the four-sigma-electron four-center H_2I_2 saddle points is investigated. The di-substituted molecule $C_2H_2Cl_2$ is examined to obtain a feeling for the capability of the model to describe multi-substituted molecules.

Net atomic charges, dipole moments, bond strengths, and ionization potentials are derived from the computed molecular wave function for each molecule considered.

Some effects of varying the integral approximation expressions and input atomic data are examined in Chapter V.

Chapter VI is an assessment of the selected valence electron model at the presently reported stage of its development.

CHAPTER II

DEVELOPMENT OF THE MODEL

Specifications

The model consists of the use of a Hartree-Fock SCF-LCAO-MO wave function Ψ to describe those molecular properties determined by a subset of the valence electrons. Definition of Ψ requires a set of one-center basis functions. Computation of the adjustable molecular orbital parameters (LCAO-MO expansion coefficients) in Ψ by the variational method results in the need to evaluate numerous integrals over these basis functions[1]. No integral is arbitrarily neglected.

Every carbon atom in a planar pi-moiety has an explicitly considered pi-electron which is described by a 2p atomic orbital function (AO) centered at the nuclear position and directed perpendicular to the plane of the molecule. A selected carbon sigma electron is represented by a 2p or a 2tr AO directed along the experimental equilibrium C-X bond direction. Each substituent atom X considered is characterized by a single AO representing one of its valence electrons; such sigma AO's are directed toward the substituted carbon corresponding to the substituent atom.

In the model of H_2I_2 each atom is represented by a single valence electron. Hydrogen is assigned a 1s AO and iodine a 5p AO directed at the nearest hydrogen. The orbitals describing one electron of each atom in the diatomics HX are directed towards the core of the other atom.

All non-explicitly considered electrons on a given atom, together with the nucleus, are taken to be a non-polarizable core located at the nuclear position. A core electron is assumed to exactly cancel one unit of nuclear charge. The core of atoms having substituents not explicitly considered is taken to include those substituents. For example, the core of a non-substituted benzene ring carbon consists of the nucleus, the two inner shell 1s and three valence sigma electrons, and the attached hydrogen atom.

Selected valence electron models for mono-substituted ethene and benzene and for H_2I_2 are illustrated by Figures 1-3, respectively.

Integral Evaluation

The restriction of attention to some of the valence electrons together with the use of an approximate wave functional form produces an uncertain foundation for the description of molecular properties. These drawbacks are largely compensated in the model by the use of integral approximation expressions and atomic data. First, the AO's employed are the Slater[34]-Zener[35] orbitals (SZO's),

$$\chi_{n\ell m} = N\, r^{n^*-1}\, e^{-\zeta r}\, Y_\ell^m(\theta,\phi), \qquad (1)$$

where N is a normalization constant and Y_ℓ^m is the spherical harmonic function. The parameters n* and ζ were adjusted by Slater[34] to obtain agreement with empirical values of stripped atom and x-ray energy levels and sizes. Hybrid orbitals are taken as the normalized linear combinations of SZO's

$$X = \chi_{n00}/a + \chi_{n10}\,(a^2-1)^{\frac{1}{2}}/a, \qquad (2)$$

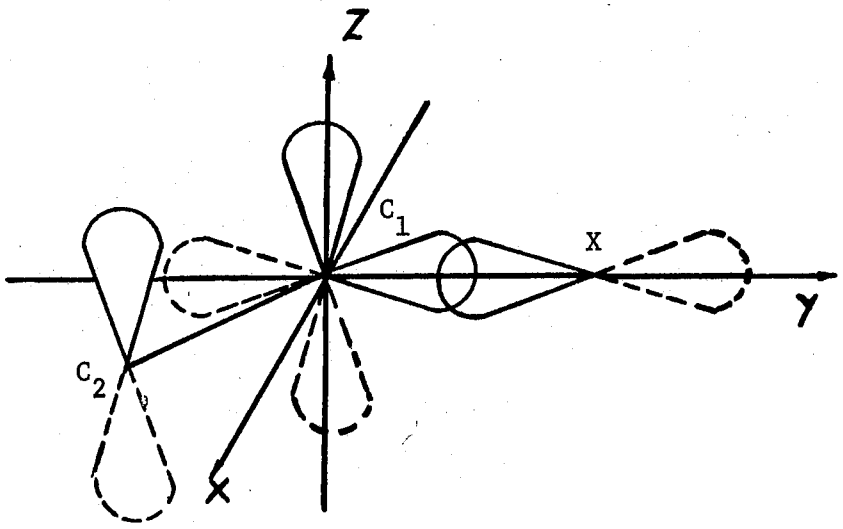

Figure 1. Schematic of a Selected Valence Electron Model for C_2H_3X

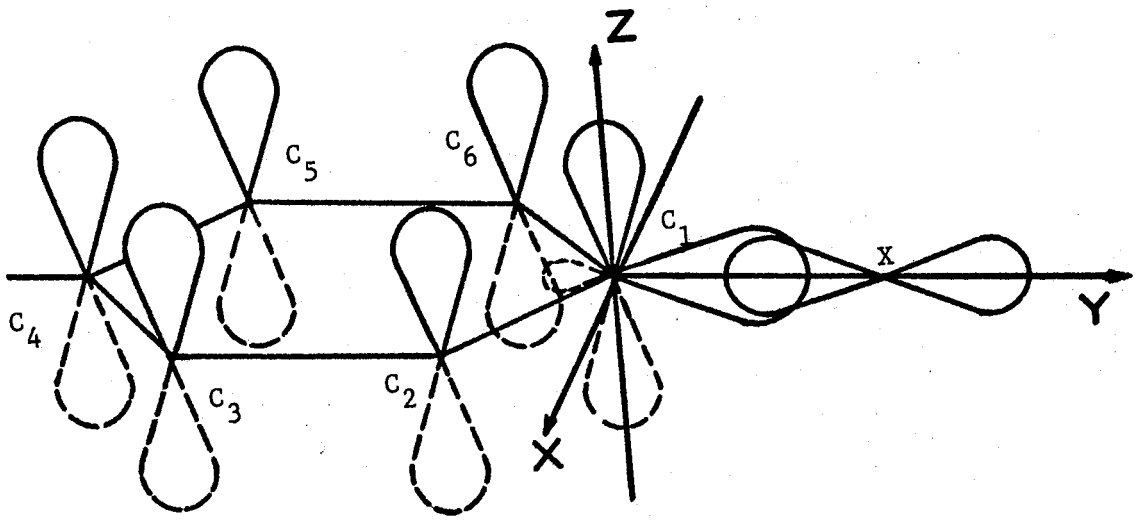

Figure 2. Schematic of a Selected Valence Electron Model for C_6H_5X

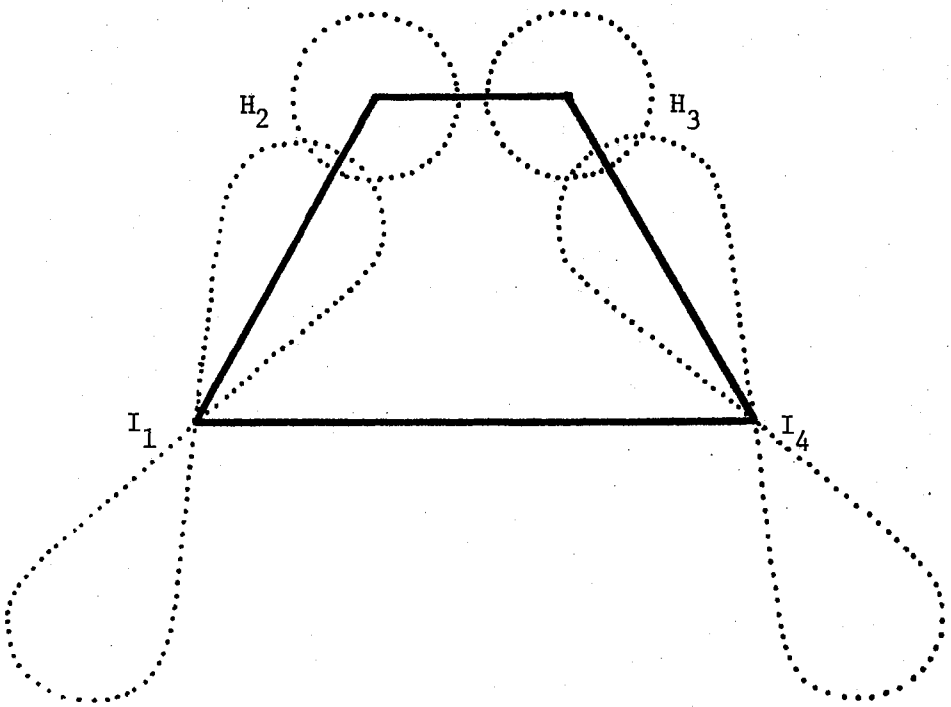

Figure 3. Schematic of a Selected Valence Electron Model for H_2I_2

where a is $\sqrt{2}$, $\sqrt{3}$, or $\sqrt{4}$ for di, tr, or te hybridizations, respectively.

Second, the integrals involving the SZO's are evaluated by means of several experience-guided procedures. The overlap integral $S_{pq} = \langle \chi_p | \chi_q \rangle$ is evaluated analytically by use of the equations of Mulliken, Rieke, Orloff, and Orloff[36]. Those of their formuli used were first checked and corrected for sign where necessary. The one-center core-attraction integral

$$\begin{aligned} \rho_p &= \langle \chi_p^1 | Z_a^c / r_{1a} | \chi_p^1 \rangle \\ &= - Z_a^c \, \zeta_p / n_p^*, \end{aligned} \tag{3}$$

where Z_a^c is the core charge assigned to the atom a on which χ_p is centered, is also evaluated analytically. All other integrals are evaluated by use of the integral approximation expressions credited to Goeppart-Mayer and Sklar[37], Mulliken[38], Pople[7], and Pariser[39]. These expressions are given by Equations (4), (5), (6)-(7), and (8), respectively:

$$(-\tfrac{1}{2}\nabla_1^2 + V_{1a}) | \chi_p^1 \rangle \cong - \mathrm{VSIP}_p | \chi_p^1 \rangle, \qquad \chi_p \text{ centered on a;} \tag{4}$$

$$\chi_p^1 \chi_q^1 \, d\tau_1 \cong \tfrac{1}{2} \langle \chi_p | \chi_q \rangle \, (\chi_p^1 \chi_p^1 + \chi_q^1 \chi_q^1) \, d\tau_1; \tag{5}$$

$$\langle \chi_p^1 | V_{1a} | \chi_p^1 \rangle \cong - Z_a^c / R_{ab}, \qquad \chi_p \text{ centered on b} \neq \text{a;} \tag{6}$$

$$\langle \chi_p^1 \chi_q^2 | 1/r_{12} | \chi_p^1 \chi_q^2 \rangle = (pp|qq) \cong 1/R_{ab}; \tag{7}$$

$$\langle \chi_p^1 \chi_p^2 | 1/r_{12} | \chi_p^1 \chi_p^2 \rangle = (pp|pp) \cong VSIP_p + VSEA_p . \tag{8}$$

In these equations $V_{1a} = -Z_a^c/r_{1a}$ and $VSIP_p$ and $VSEA_p$ are abbreviations for the valence-state ionization potential and electron affinity assigned to atomic orbital χ_p.

Evaluation of the integrals

$$H12_{pq} = \langle \chi_p^i | -\tfrac{1}{2}\nabla_i^2 + V_{ia} + V_{ib} | \chi_q^i \rangle \tag{9}$$

and

$$H12_{qp} = \langle \chi_q^i | -\tfrac{1}{2}\nabla_i^2 + V_{ia} + V_{ib} | \chi_p^i \rangle \tag{10}$$

by use of Equations (3) through (6) gives two different results if χ_q is centered on atom b and χ_p on a different atom a. $H12_{pq}$ must equal $H12_{qp}$ as the operator

$$H_{iab} = -\tfrac{1}{2}\nabla_i^2 + V_{ia} + V_{ib} \tag{11}$$

is Hermitian[1]. To remove this incongruity, the integrals $H12_{pq}$ and $H12_{qp}$ are replaced by

$$\begin{aligned} H12_{pq}' &= H12_{qp}' \\ &= \tfrac{1}{2}(H12_{pq} + H12_{qp}) \end{aligned} \tag{12}$$

wherever they occur[21].

The atomic data for neutral atoms and the SZO parameters used in

this study are displayed in Table I. The Hinze and Jaffe'[40] (HJ hereafter) data is used except where Pritchard and Skinner[41] (PS hereafter) data is specifically acknowledged. For atoms represented in the model by more than one valence electron, the valence-state ionization potential for an electron in orbital χ_p is taken as the neutral atom experimental value, $VSIP_a(1)$, plus the sum of its repulsion interactions with the other $(\ell-1)$ explicitly considered electrons on the same atom a. The repulsion energy is taken as the mean of the n one-orbital integrals $(pp|pp)$ on a. Thus,

$$VSIP_a(Z_a^c) = VSIP_a(1) + \frac{\ell-1}{n} \sum_{p(a)}^{n} (pp|pp), \qquad (13)$$

where ℓ is the number of electrons contributed to the model molecule by atom a. The summation term of Equation (13) is subtracted from $VSEA_a(1)$ to obtain $VSEA_a(Z_a^c)$.

Equation (13) is used in this study to approximate $VSIP_C(Z_C^c)$ whenever $Z_C^c > 1$ for two reasons. First, third electron valence-state ionization potentials are not available from Hinze and Jaffe's[40] papers. The other reason is that values for the second valence-state ionization potential computed by Equation (13) for C^+ trtr$\underline{\text{tr}}$ and trtr$\underline{\pi}$ states (28.02 and 23.56 e.V., respectively) are very close to those reported by Hinze and Jaffe' (28.14 and 23.68 e.V., respectively).

The overlap integrals involving bromine, for which $n^* = 3.7$, are evaluated by replacing $r^{n^*-1} = r^{2.7}$ in χ by the sum $(a_1r^1 + a_2r^2 + a_3r^3)$. Thus the 4p SZO is taken as a linear combination of 2p, 3p, and 5p orbitals having the value of ζ assigned to bromine (2.054). The coefficients a_i are determined by a least-squares fit to $r^{2.7}$ over the range

TABLE I

ATOMIC DATA AND SZO PARAMETERS

Atom	Configuration	Orbital	Hinze and Jaffe VSIP (eV)	Hinze and Jaffe VSEA (eV)	Pritchard and Skinner VSIP (eV)	Pritchard and Skinner VSEA (eV)	n*	ζ (au^{-1})
H	S	1s	13.60	-0.75	13.60	-0.75	1	1.000
C	trtrtrp	2tr	15.62	-1.95			2	1.625
		2p	11.16	-0.03			2	1.625
F	$s^2p^2p^2p$	2p	20.86	-3.50	20.98	-3.65	2	2.600
Cl	$s^2p^2p^2p$	3p	15.03	-3.73	15.09	-3.82	3	2.033
Br	$s^2p^2p^2p$	4p	13.10	-3.70	13.72	-3.69	3.7	2.054
I	$s^2p^2p^2p$	5p	12.67	-3.52	12.61	-3.55	4	1.900

0.1 to 6.1 Å. The values found for a_1, a_2, and a_3 are -0.7694, 1.2157 $Å^{-1}$, and 0.4037 $Å^{-2}$, respectively. Values computed for the overlap of a carbon 2tr and 2p with a bromine 4p are displayed in Table II.

Wave Functional Forms and SCF Equations

Both restricted and unrestricted LCAO-MO wave functional forms and their corresponding SCF equations are used. The restricted formalism is found to be sufficient at near equilibrium bond distances and is less expensive in terms of computer time than the unrestricted formalism. The latter must be used to properly describe bond separation to neutral molecular fragments.

Restricted LCAO-MO-SCF Formalism

The restricted LCAO-MO-SCF equations are the closed shell equations of Roothaan[42]. The total energy wave equation

$$H\Psi = E_e\Psi \tag{14}$$

is approximated with the Hamiltonian

$$H = \sum_{i}^{N} -\tfrac{1}{2}\nabla_i^2 + \sum_{i}^{N}\sum_{a}^{\text{atoms}} V_{ia} + \sum_{i<j}^{N} 1/r_{ij}, \tag{15}$$

where $V_{ia} = -Z_a^c/r_{ia}$ and Z_a^c = core charge assigned to atom a, and with the approximate wave functional form

$$\Psi = A \prod_{m=1}^{N_m} \phi_m(i)\ \alpha(i)\ \phi_m(i+1)\ \beta(i+1), \tag{16}$$

where $i = 2m - 1$, the total number of electrons $N = 2N_m$, A is the elec-

TABLE II

APPROXIMATE CARBON-BROMINE OVERLAP INTEGRAL VALUES

R (Å)	S(C-Br) 2tr-4p	2tr-2p	2tr-3p	2tr-5p
1.50	0.5665	0.3983	0.5281	0.5722
1.75	0.5265	0.3063	0.4482	0.5385
2.00	0.4380	0.2170	0.3463	0.4559
2.25	0.3359	0.1448	0.2496	0.3566
2.50	0.2420	0.0923	0.1705	0.2623
2.75	0.1659	0.0567	0.1115	0.1835
	2p-4p	2p-2p	2p-3p	2p-5p
1.00	0.0062	0.2456	0.1584	0.0066
1.25	0.2287	0.3178	0.3165	0.2193
1.50	0.3398	0.2981	0.3583	0.3310
1.75	0.3575	0.2389	0.3272	0.3558
2.00	0.3180	0.1737	0.2640	0.3239
2.25	0.2542	0.1179	0.1957	0.2652
2.50	0.1882	0.0760	0.1362	0.2011
2.75	0.1316	0.0471	0.0904	0.1438
3.00	0.0879	0.0283	0.0576	0.0981
3.25	0.0565	0.0165	0.0356	0.0644

tron antisymmetrization operator averaging Ψ over permutations P,

$$A = (N!)^{-\frac{1}{2}} \sum_{P} (-1)^{P} P, \tag{17}$$

and the ϕ_m are the LCAO-MO's in terms of the basis function atomic orbitals

$$\phi_m = \sum_{p}^{AO's} C_{pm} \chi_p . \tag{18}$$

The minimization of the total electronic energy

$$E_e = \langle \Psi | H | \Psi \rangle \tag{19}$$

with respect to the LCAO-MO coefficients C_{pm} subject to the requirements

$$\langle \phi_m | \phi_m \rangle = 1, \quad m = 1, N_m \tag{20}$$

gives the matrix secular equation

$$F\ C = S\ C\ \epsilon \tag{21}$$

for the C_{pm} and the molecular orbital energies ϵ_m. The basis function matrix elements for F and S in Equation (21) are given in Equations (22) - (26):

$$F_{pq} = Hl_{pq} + G_{pq} , \tag{22}$$

$$Hl_{pq} = \langle \chi_p^i | -\tfrac{1}{2}\nabla_i^2 + \sum_a V_{ia} | \chi_q^i \rangle , \tag{23}$$

$$G_{pq} = \sum_{u,v}^{AO's} P_{uv} \left[(pq|uv) - \tfrac{1}{2}(pu|qv) \right] , \tag{24}$$

$$P_{uv} = 2 \sum_{m}^{occ} C_{um} C_{vm}, \tag{25}$$

$$S_{pq} = \langle \chi_p^i | \chi_q^i \rangle . \tag{26}$$

The total energy is then, in terms of integrals over the basic functions,

$$E_e = \tfrac{1}{2} \sum_{pq}^{AO's} P_{pq} [Hl_{pq} + F_{pq}]. \tag{27}$$

Equation (21) is solved by iteration. A starting C matrix is obtained by solution of a Hückel problem; F_{pq} is taken as $\frac{1}{2}(VSIP_p(1) + VSIP_q(1))$ for this purpose. C_{pq} values are required to converge to within ±0.00005.

Unrestricted LCAO-MO-SCF Formalism

The unrestricted LCAO-MO-SCF equations are those of Pople and Nesbet[43]. The total energy wave function

$$H\Psi = E_e\Psi \tag{28}$$

is approximated with the Hamiltonian

$$H = Hl + H2 \tag{29}$$

where

$$Hl = \sum_{i}^{N} (-\tfrac{1}{2}\nabla_i^2 + \sum_{a}^{atoms} V_{ia}), \tag{30}$$

$$V_{ia} = -Z_a^c / r_{ia}, \tag{31}$$

$$Z_a^c = \text{core charge assigned to atom a,} \tag{32}$$

$$H2 = \sum_{i<j}^{N} 1/r_{ij}, \tag{33}$$

and with the approximate wave functional form

$$\Psi = A\left[\prod_{m=1}^{N_\alpha} \psi_m^\alpha(m) \prod_{n=1}^{N_\beta} \psi_n^\beta(n)\right], \tag{34}$$

where the total number of electrons $N = N_\alpha + N_\beta$, and m and n serve double duty as molecular spin orbital and electron indices, A is the electron antisymmetrization operator which makes Ψ an average over all possible permutations P of the electrons

$$A = [(N_\alpha + N_\beta)!]^{-\frac{1}{2}} \sum_P (-1)^P P \tag{35}$$

and the ψ_m^s are LCAO molecular spin orbitals (MSO's)

$$\psi_m^s = \phi_m^s \eta_m^s \tag{36}$$

$$\phi_m^s = \sum_p^{AO's} C_{pm}^s \chi_p \tag{37}$$

$$\eta_m^s = \alpha \text{ if } s = 1; \ \beta \text{ if } s = 2. \tag{38}$$

The minimization of the total electronic energy with respect to the LCAO-MSO coefficients C_{pm}^s subject to the requirements

$$\langle\psi_m^s|\psi_m^s\rangle = \langle\phi_m^s|\phi_m^s\rangle = 1, \quad m = 1, N_s \tag{39}$$

for $s = \alpha$ and $s = \beta$ gives the matrix secular equations

$$F^s C^s = S C^s \varepsilon^s, \quad s = \alpha,\beta \tag{40}$$

for the C^s_{pm} and the spin orbital energies ε^s_m. The basis function matrix elements for F^s and S are by Equations (41) to (46):

$$F^s_{pq} = Hl_{pq} + G^s_{pq}, \tag{41}$$

$$Hl_{pq} = \langle \chi^i_p | -\tfrac{1}{2}\nabla^2_i + \sum_a V_{ia} | \chi^i_q \rangle , \tag{42}$$

$$G^s_{pq} = \sum_{u,v}^{AO's} [P_{uv}(pq|uv) - P^s_{uv}(pv|uq)] , \tag{43}$$

$$P^s_{uv} = \sum_m^{occ} C^s_{um} C^s_{vm} , \tag{44}$$

$$P_{uv} = P^\alpha_{uv} + P^\beta_{uv} , \tag{45}$$

$$S_{pq} = \langle \chi^i_p | \chi^i_q \rangle . \tag{46}$$

The total electronic energy E is then

$$E_e = \tfrac{1}{2} \sum_{pq}^{AO's} P^s_{pq}(Hl_{pq} + F^s_{pq}). \tag{47}$$

The solution--molecular spin orbital functions and energies--of Equation (40) is obtained by using the following procedure. A Hückel solution C is obtained as described above in the section on the restricted formalism. Both C^α and C^β are equated to C. Then a new $C^\alpha(C^\beta)$ matrix is obtained by solution of Equation (40) with $s = \alpha$ ($s = \beta$) while $C^\beta(C^\alpha)$ is held constant. This alternating process is repeated until every new C^s_{pq} equals its value at the beginning of the two-step cycle to with ±0.00001.

Test computations show that for energies E_e, ε_m, and ε^s_m accurate to

0.0001 e.V. the MO and MSO coefficients C_{pm} and C^{s}_{pm} must be found to within ±0.00001 by iterative solution of Equation (21) or Equation (40). These equations are solved by simple matrix manipulation and the Jacobi matrix diagonalization method[44].

Net Atomic Charge and Partial Overlap Population

Following Mulliken[45] a population analysis of the P_{pq} gives Equations (48) and (49) for the net atomic charge Q_a and the bond partial overlap population POP_{ab}, respectively.

$$Q_a = Z^c_a - \sum_{p(a)}^{AO's} \sum_{q} P_{pq} S_{pq} \tag{48}$$

$$POP_{ab} = \sum_{p(a)}^{AO's} \sum_{q(b)} P_{pq} S_{pq} \tag{49}$$

These quantities are indices of charge transfer and bond strength with respect to the separated neutral atoms that are of value in the determination of relative reactivity of various sites within a molecule or a series of molecules[45].

Molecular Energy and Core Repulsion

The determination of the equilibrium bond properties requires a consideration of core repulsion between the separate molecular fragments. The molecular energy E_m is given by the sum of the molecular electronic energy E_e and core repulsion energy E_{cr},

$$E_m = E_e + E_{cr}. \tag{50}$$

The core repulsion expression is

$$E_{cr} = \sum_{a<b} Z_a^{cr} Z_b^{cr}/R_{ab} \tag{51}$$

$$= \sum_{a<b} V_a^{cr} V_b^{cr} R_{ab}, \tag{52}$$

where $V_a^{cr} = Z_a^{cr}/R_{ab}$ and the Z_a^{cr} are effective core charges for the specific purpose of evaluating E_{cr}. Only those terms for atoms that are moved with respect to one another are retained in E_{cr}.

In this study V_a^{cr} is obtained from a single exponential fit to the absolute value of the Herman-Skillman[46] tabulated values of the Hartree-Fock-Slater last-valence-electron potential for atom a. The functional form for V_a^{cr} is

$$V_a^{cr}(R) = (Z_a^c + (Z_a^n - Z_a^c) \exp(-D_a R))/R, \tag{53}$$

where Z_a^c is the assigned core charge for computation of E_e and Z_a^n is the nuclear charge of atom a. The value of D_a is determined in this thesis by a least-squares criterion fit to tabulated points before and after the Latter cut-in distance R_L.[46]

For $R \geq R_L$ the one-electron potential computed by Herman and Skillman is equal to 1/R. The discontinuity is not significant in the atomic calculations[46]. But for molecules the value of R_L for bonded atoms is near the equilibrium bond length. Therefore, the cut-in region points are omitted in the fitting procedure so as to obtain parameters dependent upon the more reliable inner points before and outer points after the discontinuous cut-in region. The cut-in region is taken to be the three points immediately before and the three after $R = R_L$.

Values of exponential parameter D_a of Equation (53) for carbon, fluorine, chlorine, bromine, and iodine are given in Table III as determined (a) by a 10-10 fit to the 13th-4th inner and 4th-13th outer tabulated points, (b) by a 5-5 fit to the 8th-4th inner and 4th-8th outer points, and (c) assumption.

For atoms assigned a core charge Z_a^c value of 1, the above described values of D_a are used. For atoms assigned larger core charge values, D_a is modified as to have a smaller fraction of $(Z_a^n - Z_a^c)$ in Equation (53). This modification is in accordance with the idea that the remaining electrons shield their respective nuclear charges more efficiently in the case $Z_a^c > 1$. The modification expression suggested by Pohl[25,47] is used, viz.

$$D_{ai} = D_{a1} (Z_a^n - S_a^i)/(Z_a^n - S_a^1) \tag{54}$$

where $i = Z_a^c$ and S_a^i is the Slater shielding constant[34] for the ith to last valence electron. For example, for carbon with an assigned core charge of 2, use of the 10-10 value for D_{c1} gives

$$D_{c2} = D_{c1}(3.60)/(3.25) = 3.7390 \text{ Å}^{-1} . \tag{55}$$

Values for D_{c2} and D_{c3} are presented with the D_{a1} values in Table III.

Bond Energy

The bond energy E_b is computed as the difference between the molecular energy and the unrestricted computed values for the infinitely separated molecular fragment energies E_f,

$$E_b = E_m - E_f . \tag{56}$$

TABLE III

CORE REPULSION EXPONENTIAL PARAMETERS IN INVERSE ANGSTROM UNITS

Set Ideogram	Atom	D_{a1}	D_{a2}	D_{a3}
10-10	C	3.3755	3.7390	4.1025
	F	4.3788		
	Cl	3.4401		
	Br	4.1342		
	I	3.6824		
5-5	C	3.3893	3.7543	4.1193
	F	4.5118		
	Cl	3.3830		
	Br	3.6200		
	I	3.3896		
Assumption	H	3.3850		
	F	3.3850		
	Br	3.3850		

Equilibrium Bond Length, Energy, Force Constant, and Stretching Frequency

An exact matching fit of the functional form

$$E_m = \sum_{i=o}^{n} a_i r^i \tag{57}$$

is made to calculated values of E_m or E_b at r values spaced by 0.25Å. Use of 5 to 10 points (E_m,r) was found to correctly predict the model results to within 0.01Å for the bond length, 0.01 e.V. for the bond energy, and 20 cm^{-1} for the stretching frequency. The stretching frequency is determined by a molecular fragment approximation:

$$\nu = (K/M_r)^{\frac{1}{2}}/2\pi, \tag{58}$$

where K, the bond force constant, is the second derivative of the fitted function E_m at the calculated equilibrium distance and M_r is the reduced mass of the molecular fragments joined by the considered bond. Computed frequencies are not quantitatively comparable to any normal modes of vibration as all atoms save one or two are not allowed to move with respect to one another. However, qualitative comparisons with the modes primarily determined by C-X stretch are possible.

Model Molecular Dipole Moment

The dipole moment

$$\mu = \mu_x \bar{i} + \mu_y \bar{j} + \mu_z \bar{k} \tag{59}$$

is computed in an approximate manner from the electron density matrix

P_{pq} and the overlap integrals S_{pq}. By definition, along the coordinate Y

$$\mu_y = \sum_i^{elec} -e \langle\Psi|y^i|\Psi\rangle + \sum_a^{atoms} Z_a^c \, e \, Y_a \tag{60}$$

where

$$\begin{aligned} \sum_i \langle\Psi|y^i|\Psi\rangle &= \sum_m^{occ} N_m \langle\phi_m^i|y^i|\phi_m^i\rangle \\ &= \sum_{pq}^{AO's} P_{pq} \langle\chi_p^i|y^i|\chi_q^i\rangle \end{aligned} \tag{61}$$

With N_m being the occupancy number, 1 or 2, of molecular orbital m. Atomic orbitals χ_p and χ_q are centered on atoms a and b, respectively.

Approximate Evaluation

Following the reasoning of Dewar[48] and of Davies[49] that the integral $\langle\chi_p^i|y^i|\chi_q^i\rangle$ is proportional to the mean position of atoms a and b and to the overlap of the AO's p and q, the approximation

$$\langle\chi_p^i|y^i|\chi_q^i\rangle \cong \tfrac{1}{2}(Y_a + Y_b) \, S_{pq} \tag{62}$$

is made. This simplification reduces Equations (60) and (61) to

$$\begin{aligned} \mu_y \cong -e \sum_{pq}^{AO's} P_{pq} \, S_{pq} (\tfrac{1}{2}(Y_a + Y_b)) \\ + e \sum_a^{atoms} Z_a^c \, Y_a \, . \end{aligned} \tag{63}$$

Replacement of y with x or z gives the corresponding expressions for the remaining components of the model molecular dipole moment. It is notable that Equation (62) is the same as is obtained by use of the Mulliken ap-

proximation.

Analytic Evaluation

The approximation inherent in Equation (63) may be seen by rigorous evaluation of Equation (60). Let

$$y^i = Y_c + y_c^i, \tag{64}$$

where y^i and Y_c are the y coordinants of electron i and atom c, respectively, in the master coordinant system. y_c^i is the y coordinant of electron i in the local coordinate system of atom c. Using Equations (60) and (64) with c taken as the atom on which the left orbital in the integral $\langle \chi_r | y | \chi_s \rangle$ is centered, the electronic component of μ_y may be written as

$$-e \sum_{pq}^{AO's} P_{pq} \langle \chi_p^i | Y_a + y_a^i | \chi_q^i \rangle = -e \sum_{pq}^{AO's} P_{pq} S_{pq} Y_a - e \sum_{pq}^{AO's} P_{pq} \langle \chi_p^i | y_a^i | \chi_q^i \rangle \tag{65}$$

Since $(P_{pq}S_{pq}Y_a + P_{qp}S_{qp}Y_b) = (\frac{1}{2}P_{pq}S_{pq}(Y_a + Y_b) + \frac{1}{2}P_{qp}S_{qp}(Y_b + Y_a))$, the first terms of Equations (65) and (63) are identical. The approximate Equation (63) for μ_y lacks only the second term on the right of Equation (65). This term may be seen to be small by simply choosing local Cartesian coordinate systems for atoms a and b parallel to the master and noting that the integral $\langle \chi_p^i | y_a^i | \chi_q^i \rangle$ is zero by symmetry if p = q. Noting that

$$\langle \chi_p^i | y_a^i | \chi_q^i \rangle + \langle \chi_q^i | y_b^i | \chi_p \rangle = \langle \chi_p^i | y_a^i + (-Y_{ab} + y_a^i) | \chi_q \rangle, \tag{66}$$

where $Y_{ab} = |Y_a - Y_b|$, and making the coordinant change

$$y^i_{am} = y^i_a - \tfrac{1}{2} Y_{ab} , \tag{67}$$

the second term on the right-hand side of Equation (65) may be written as

$$\begin{aligned} \Delta\mu_y &= -e \sum_{pq}^{AO's} P_{pq} \langle \chi^i_p | y^i_a | \chi^i_q \rangle \\ &= -2e \sum_{p<q}^{AO's} P_{pq} \langle \chi^i_p | y^i_{am} | \chi^i_q \rangle . \end{aligned} \tag{68}$$

For the selected-valence model in this study this summation simplifies to

$$\Delta\mu_y = -2e P_{pX} \langle \chi^i_p | y^i_{am} | \chi^i_X \rangle \tag{69}$$

for the monosubstituted planar pi-moiety molecules (χ_p = substituted carbon sigma AO) and for the hydrogen halides ($\chi_p = \chi_H$), if y is the coordinant along the line through the positions of atom a and halogen atom X. Values of $\Delta\mu_y$ for C_2H_3F and HF are compared with the value of μ_y given by Equation (63) later in the thesis and found to be approximately 0.04 (about 1% change) and 0.2 (about 7% change) Debye, respectively, at near equilibrium C-F and H-F bond lengths. Thus, Equation (63) is a good approximation for the molecules examined in this study.

Computation

A computer programme system was developed to perform the calculations described in this chapter.

The overlap computing subprogrammes successfully reproduce results

reported in the literature[21,26,36]. The Jacobi matrix diagonalization subprogramme system correctly handles a 8x8 National Bureau of Standards test matrix reported by Rosser, et al.[50], and included by Gregory and Karney[51] in their collection of test matrices.

Experience with the computations shows that for molecules having bonding atoms within about .5Å of their equilibrium separation, the restricted and unrestricted wave functions and energies are equivalent to 5-10 significant digits. Thus, the programme system can be checked against the unrestricted results of Harris and Pohl[22] for the hydrogen halides. They employed the same set of integral approximations as given in Equations (4) through (12). The PS atomic data is used for HX as did Harris and Pohl. This set of approximations requires a complex unrestricted wave function for diatomics at small internuclear distances, while the restricted wave function remains real. No complex wave functions are encountered in either restricted or unrestricted computations described in this thesis except in the diatomic HX case.

The comparison of electronic energies and dipole moments is made in Table IV. It is clear that the programme correctly reproduces the Harris-Pohl results near equilibrium. The slight differences are due to use of somewhat different values for unit conversion factors (see Appendix). As expected, at large separation the restricted wave function tends to the ionic form ($H^+ + X^-$) with energy ($-VSIP_X + VSEA_X$) instead of to (H + X) with the lower neutral model atom energy ($-VSIP_H - VSIP_X$).

Table V shows the highest occupied molecular orbital energy I_m, the model molecular dipole moment μ, and the bond properties determined by use of the 5-5 and 10-10 sets of the parameters D_a in the core repulsion expression. The corresponding experimental and Harris-Pohl computed

TABLE IV

COMPARISON OF RESTRICTED COMPUTATIONS FOR THE HYDROGEN HALIDES

WITH THE UNRESTRICTED RESULTS OF HARRIS AND POHL

Molecule	R Å	Electronic Energy (e.V.)		Dipole Moment (D)	
		Restri.	Harris-Pohl	Restri.	Harris-Pohl
HF	0.688	-66.49	-66.50	3.328	3.310
	0.917	-56.68	-56.66	3.487	3.481
	1.146	-51.26	-51.29	3.448	3.320
	1.376	-47.47	-47.70	3.702	3.055
	1.605	-44.54	-45.09	4.124	2.514
	1.834	-42.21	-43.21	4.615	1.662
HCl	0.956	-49.21	-49.29	3.815	3.500
	1.275	-43.64	-43.64	2.210	2.189
	1.594	-40.12	-40.32	2.170	1.879
	1.913	-37.30	-37.85	2.476	1.629
	2.231	-34.99	-36.00	2.905	1.164
	2.550	-33.09	-34.72	3.368	0.629
HBr	1.061	-45.18	-45.29	2.884	2.573
	1.414	-40.70	-40.68	1.524	1.505
	1.768	-37.54	-37.75	1.568	1.317
	2.121	-34.89	-35.48	1.847	1.118
	2.475	-32.66	-33.81	2.214	0.742
	2.828	-30.87	-32.68	2.598	0.358
HI	1.203	-41.79	-41.81	1.365	1.342
	1.604	-37.94	-38.04	0.928	0.869
	2.005	-34.98	-35.38	1.031	0.821
	2.406	-32.46	-33.30	1.257	0.681
	2.807	-30.36	-31.79	1.529	0.404
	3.208	-28.71	-30.86	1.797	0.203

TABLE V

RESTRICTED RESULTS FOR THE HYDROGEN HALIDES

Method	Molecule	R_e (Å)	E_b (e.V.)	k (md/Å)	μ (D)	I_m (e.V.)
5-5	HF	0.881	-4.01	5.97	3.46	20.7
	HCl	1.490	-1.82	2.96	2.18	15.3
	HBr	1.633	-1.74	2.95	1.55	14.4
	HI	1.837	-1.34	2.60	0.99	13.5
10-10	HF	0.915	-4.12	5.91	3.49	19.9
	HCl	1.475	-1.91	3.00	2.18	15.3
	HBr	1.516	-2.31	3.07	1.54	14.7
	HI	1.823	-1.41	2.63	0.97	13.5
Harris-Pohl	HF	0.87	-5.6	5.6	3.48	
	HCl	1.44	-2.9	3.8	1.98	
	HBr	1.63	-2.5	2.5	1.36	
	HI	1.88	-2.1	2.0	0.86	
Expmt.	HF	0.917	-5.81	9.66	1.91	17.7
	HCl	1.275	-4.43	5.16	1.08	13.8
	HBr	1.414	-3.75	4.12	0.80	13.2
	HI	1.604	-3.06	3.14	0.42	12.8
	Ref.	(54)	(54)	(54)	(55)	(55)

values are also shown. The bond energies E_b are quite different from the Harris-Pohl calculation; this situation is due to the difference in the procedure for evaluating core repulsion from the Herman-Skillman tables. The results for the HX series correlate with experiment qualitatively except for the 10-10 results for HBr. The agreement with the Harris-Pohl results is semiquantitative.

The dipole correction term $\Delta\mu$ for HF at a 0.917Å separation of the atoms increases μ by 0.23 Debye or 6.7% of the approximate value (3.490) in Table IV.

Fixed Fragment Geometry

Throughout this study the experimental geometries are assumed except where bond lengths or angles are specified as varying. While this source of input molecular information may be considered to be a calibration from the standpoint of computations based solely on the properties of electrons and nuclei, it is not a particularly contraining restriction for a valence electron model. For in such models the electronic energy is determined by evaluation of its component integrals in terms of valence electron experimental data. It is not inconsistent with such an approach to assume standard bond lengths and angles from a consideration of known molecular geometries wherever such quantities are not varied. Such an approach is common[52,53]. The experimental configurations are used in this study instead of a standard set because only a few molecules are considered and it will be of interest to examine changes which result when subsequent results are obtained for the slightly different standard geometries.

CHAPTER III

COMPUTATIONS FOR THE MONO-HALOGEN SUBSTITUTED SERIES C_2H_3X, C_2HX, C_6H_5X

The capability of the model developed in Chapter II to predict properties and correlations determined by pi-electrons and substitution bonds is examined in this chapter. This capability can be explored by application to some monosubstituted pi-moiety molecules. In particular, the model may be examined for its ability to account for the substituted bond lengths, angles, binding energies, and stretching frequencies for the C-X bond. Estimates may also be made of the facility with which the model wave function treats the molecular charge distribution, dipole moment, and ionization potential at the computed equilibrium C-X bond length. Thus, the information content of the pi and substituted bond sigma electrons may be assessed. The examination is made on the fluorine, chlorine, bromine, and iodine substituted ethenes, ethynes, and benzenes.

Mono Sigma Radicals

For the computation of the bond energy it is necessary to have model-computed values for the energies of the R and X neutral sigma radicals. The energy of X· is simply $-VSIP_X$. The model electronic energy for R· must be computed using the same computational procedure as for RX. Results for the ethenyl (C_2H_3), ethynyl (C_2H·), and phenyl

(C_6H_5) sigma radicals are displayed in Table VI. Values are presented for two choices of the substituted carbon sigma AO: 2p and 2tr.

In addition to the electronic energies, net atom charge Q, the pi-bond partial overlap populations POP, and the highest occupied molecular orbital energies I_m are tabulated in Table VI. The values for Q are particularly interesting. For the ethenyl and ethynyl radicals there is no appreciable charge transfer. For the phenyl radical, there occurs an extreme charge oscillation about the ring. The cause for this model defect lies in the particular integral approximations made in Chapter II. This problem is examined for cause and solution in Chapter V.

Haloethenes

All computations for the haloethenes are characterized by the use of 1.34$\overset{o}{A}$ for the C-C bond length and 120^o for the CCX bond angle[56]. These values are within experimental error of the reported C_2H_3X geometries.

A typical LCAO-MO-SCF wave function computed for the haloethenes is that of C_2H_3F at a near equilibrium C-F separation (Table VII). It is readily seen that the occupied orbitals are nodeless but that the unoccupied ones are not, as is to be expected. The occupied MO energies are somewhat large in magnitude compared to the experimental ionization potentials. All of the unoccupied orbitals are positive, contrary to Pariser-Parr-Pople pi-only computations on similar molecules[6,7].

It should be noted that the use of a carbon 2tr sigma AO produces a more covalent wave function than a 2p as judged by the relative magnitudes of the C^σ and F molecular orbital coefficients.

The variation of the unrestricted C_2H_3F wave function with the C-F

TABLE VI

PI-MOIETY SIGMA RADICAL COMPUTATIONS†

Sigma Radical	Property	2p	2tr
$C_2H_3\cdot$	E(e.V.)	- 69.532	- 75.262
	Q_1, Q_2	0, 0	same
	POP_{12}	0.425	same
	I_m(e.V.)	12.7	same
$C_2H\cdot$	E(e.V.)	-185.224	-192.224
	Q_1, Q_2	0, 0	same
	POP_{12}	0.499	same
	I_m(e.V.)	14.7	same
$C_6H_5\cdot$	E(e.V.)	-249.081	-254.811
	Q_1, Q_2, Q_3, Q_4	.7, -.8, .9, -.9	same
	$POP_{12}, POP_{23}, POP_{34}$	.326, .457, .528	same
	I_m(e.V.)	12.7	same

†See Figures 1 and 2 for clarification of the subscripts.

TABLE VII

C_2H_3F MOLECULAR ORBITAL COEFFICIENTS AND ENERGIES AT $R_{CF} = 1.25\text{Å}$

Carbon Sigma Orbital	Atomic Orbital† Atom (nℓm)	Molecular Orbital* 1	2	3	4
2p	C_1(211)	0.9801	0.3434	0.0	0.0
	C_2(211)	-0.5952	0.8511	0.0	0.0
	C_1(210)	0.0	0.0	1.0153	0.2298
	F (210)	0.0	0.0	-0.5028	0.9115
	ε_m(e.V.)	1.96	14.89	2.35	-19.26
2tr	C_1(211)	0.8905	0.5345	0.0	0.0
	C_2(211)	-0.7550	0.7131	0.0	0.0
	C_1(200&210)	0.0	0.0	0.9708	0.4601
	F (210)	0.0	0.0	-0.7830	0.7355
	ε_m(e.V.)	2.12	-13.70	1.24	-19.94

*Underlined MO's are occupied.

†See Figure 1 for clarification of the subscripts.

bond length is presented for a 2tr carbon sigma AO in Table VIII in the summarized form of Q's and POP's. The charge variations from $R_{CF} = .50$ to $R_{CF} = 2.75\text{Å}$ indicate the wave function goes from completely ionic to entirely covalent over this range. The partial overlap populations, which may be considered to indicate bond strength, show a maximum value for the C-C pi bond at large R_{CF} and for the C-F sigma bond at R_{CF} about 1.25Å. Since the C-X overlap has its maximum value at about 1.00Å but the computed and experimental bond lengths R^{e}_{CF} are slightly greater than 1.25Å, maximum overlap does not coincide with equilibrium bond length in the present model. The maximum overlap population does. Arguments with regard to relative stabilities of molecules may be erroneous if based only on overlap considerations. This point is examined in Chapter V.

As noted in Chapter II, the restricted and unrestricted wave functions are coincident for C-X distances within $\pm 0.50\text{Å}$ of equilibrium. This coincidence is graphically displayed in Figure 4, which presents 10-10 core repulsion parameter binding curves for restricted and unrestricted electronic energies computed for C_2H_3F.

Initial computation of the C-X bond properties for the haloethene series using a 2tr carbon sigma AO and the 10-10 core repulsion parameters presented two serious difficulties. First, as may be seen from Table IX, the bond polarities for C_2H_3-Br and C_2H_3-I are contrary to expectations based on electronegativity considerations. The use of a 2p carbon sigma AO solves this problem, which results from the relative valence-state ionization potentials of the carbon 2tr and the halogen 2p atomic orbitals.

The second difficulty is the inability of the 10-10 core repulsion parameters to produce properly sequenced C-X binding energies through the

TABLE VIII

VARIATION OF NET ATOM CHARGE AND OVERLAP POPULATION WITH R_{CF} IN C_2H_3F FOR A 2TR CARBON SIGMA ORBITAL

R_{CF} (Å)	S_{CF} (2tr-2p)	Q			POP	
		C_1	C_2	F	C_1-C_2	C_1-F
0.50	-.03495	2.01	-1.00	-1.00	-.01	-.00
0.75	.26927	1.95	- .93	-1.02	.10	-.05
1.00	.38418	1.32	- .63	- .69	.31	.35
1.25	.36543	.55	- .22	- .33	.41	.49
1.50	.28849	.38	- .11	- .27	.42	.43
1.75	.20353	.26	- .05	- .21	.42	.27
2.00	.13303	.11	- .01	- .09	.43	.10
2.25	.08227	.03	- .00	- .03	.43	.04
2.50	.04879	.01	- .00	- .01	.43	.01
2.75	.02801	.00	- .00	- .00	.43	.00

TABLE IX

HALOETHENE 10-10 EQUILIBRIUM NET ATOM CHARGES

AND PARTIAL OVERLAP POPULATIONS*

Molecule	Q_a C_1	C_2	X	POP_{ab} C_1-C_2	C_1-X
C^{σ} = 2tr					
C_2H_3F	0.50	-0.19	-0.31	0.42	0.49
C_2H_3Cl	0.06	-0.01	-0.05	0.43	0.64
C_2H_3Br	-0.04	0.01	0.03	0.43	0.67
C_2H_3I	-0.06	0.01	0.05	0.42	0.66
C^{σ} = 2p					
C_2H_3F	1.73	-0.79	-0.93	0.20	0.09
C_2H_3Cl	0.69	-0.23	-0.45	0.41	0.43
C_2H_3Br	0.52	-0.16	-0.36	0.42	0.47
C_2H_3I	0.41	-0.11	-0.30	0.42	0.46

*All values are at the calculated E_b minimum region.

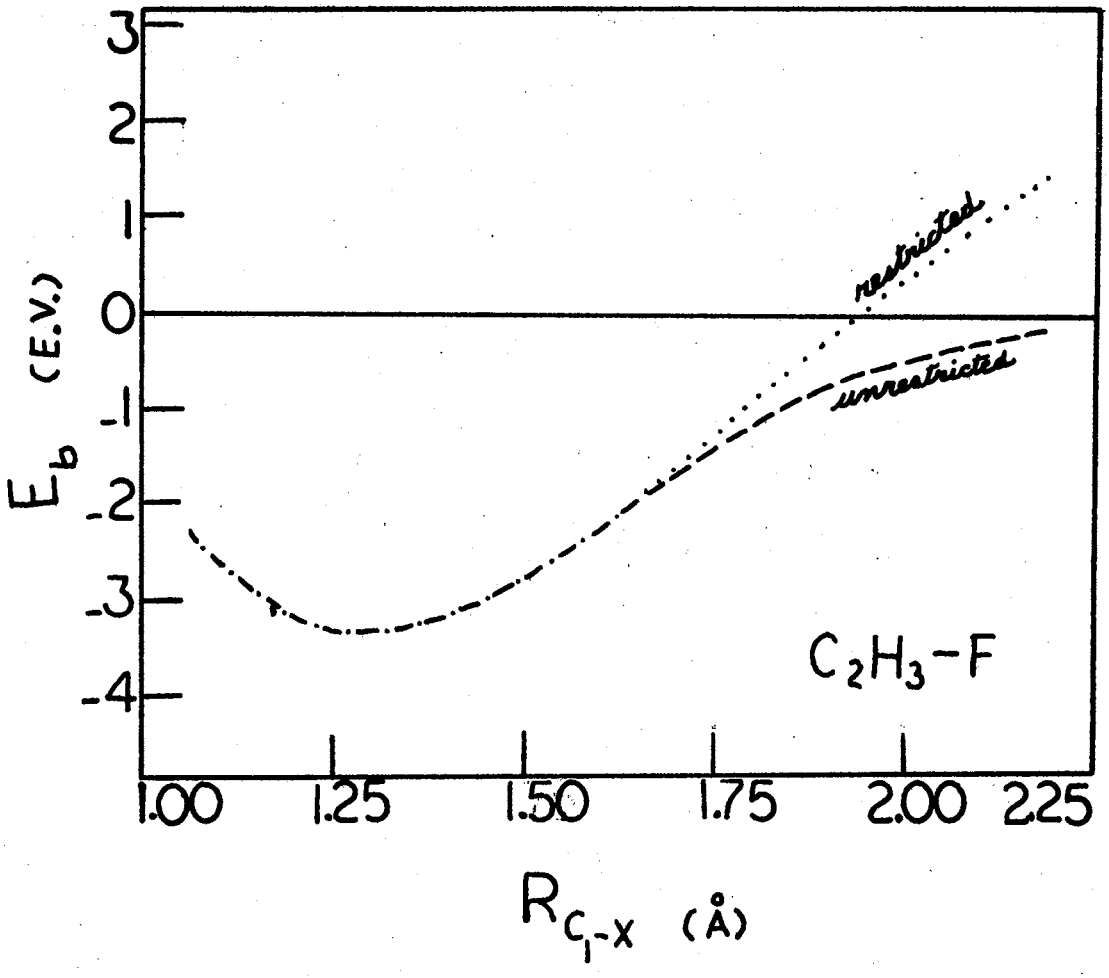

Figure 4. Comparison of Restricted and Unrestricted 10-10 Binding Curves for the C-F Bond in C_2H_3F With a 2tr Carbon Sigma Orbital

halogen series. As shown in Figures 5 and 6 and displayed in Tables X and XI, neither use of a carbon 2tr nor of a 2p sigma AO results in an electronic energy curve such that the 10-10 core repulsion produces a properly sequenced C_2H_3-Br binding energy. In the 2tr case, even C_2H_3-I is out of place. For 2p, $-E_b$ for C_2H_3-F is much too large.

An examination of the Herman-Skillman tabulated potential points shows that the 13th-9th points before the Latter cut-in distance are inside of the internuclear distance range of interest. The use of D values determined from the 8th-4th inner and 4th-8th outer points (5-5 core repulsion parameters) gives some what better results, as shown in Tables X and XI. E_b for C_2H_3-I is then properly sequenced.

The assumption that $D_{BR} = 3.385$, which is equal to the 5-5 values of D_C, D_{CL}, and D_I to three significant digits, improves the bromine situation considerably more. Even better results are obtained when the PS data are used for bromine instead of the HJ data. It is to be noted that whereas the PS and HJ data are much the same for H, C, F, Cl, and I, the VSIP's for Br differ by 0.6 e.V. (see Table I).

E_b for C_2H_3-F is also improved in the 2p carbon sigma case by the assumption that $D_F = 3.385$.

Thus, the best results for bond polarity and binding energies in the C_2H_3-X series are obtained by the use of a 2p carbon sigma AO, 5-5 core repulsion parameters for C, Cl, and I, assumption core repulsion parameters for F and Br, and PS data for Br. These results are starred in Table XI as are the best 2tr results in Table X. The best 2p binding curves are displayed in Figure 7.

Examination of the other computed properties displayed in Tables X and XI shows the model properly sequences equilibrium distances, force

TABLE X

RESULTS FOR THE HALOETHENES WITH A CARBON 2TR SIGMA ORBITAL

Method	Molecule	R_e^{cx} (Å)	E_b^{cx} (e.V.)	K^{cx} (md/Å)	ν^{cx} (cm^{-1})	μ (D)	I_m (e.V.)
10-10	C_2H_3-F	1.29	-3.4	5.3	900	1.68	13.7π
	C_2H_3-Cl	1.71	-3.1	3.4	620	.36	13.0π
	C_2H_3-Br	1.80	-3.7	3.2	520	.25	12.6π
	C_2H_3-I	1.96	-3.2	2.7	450	.49	12.5π
5-5	* C_2H_3-F	1.28	-3.5	5.1	880	1.76	13.7π
	* C_2H_3-Cl	1.73	-3.0	3.4	610	.36	13.0π
	C_2H_3-Br	1.85	-3.4	3.3	710	.26	12.6π
	* C_2H_3-I	2.04	-2.8	2.8	460	.51	12.4π
Assumption	C_2H_3-Br	1.91	-3.1	3.4	530	.27	12.6π
Assumption and PS data	* C_2H_3-Br	1.91	-2.9	3.4	530	.05	12.8π
Experiment	C_2H_3-F	1.348†	-4.4	5.6	1100	1.43	10.37
	C_2H_3-Cl	1.732	-3.4	3.4	650	1.42	10.00
	C_2H_3-Br	1.891	-2.8	2.8	560	1.42	9.80
	C_2H_3-I	2.089	-2.5	2.3	500	1.27	9.33
	Ref.	(56)	(57)#	(66)#	(58)#	(59)	(60)

*Best overall results for C^{σ} = 2tr.

#Average bond energies, force constants, and frequencies.

†Ref. (61).

TABLE XI

HALOETHENE RESULTS WITH A 2P CARBON SIGMA ORBITAL

Method	Molecule	R_e^{cx} (Å)	E_b^{cx} (e.V.)	K^{cx} (md/Å)	ν^{cx} (cm^{-1})	μ (D)	I_m (e.V.)
10-10	C_2H_3-F	1.03	-6.0	6.3	980	4.97	14.7π
	C_2H_3-Cl	1.72	-3.4	2.7	710	3.22	14.6σ
	C_2H_3-Br	1.83	-3.5	2.5	460	2.79	13.9σ
	C_2H_3-I	2.00	-2.8	2.2	410	2.60	13.1σ
5-5	C_2H_3-F	1.01	-6.4	8.5	1130	5.03	14.6π
	* C_2H_3-Cl	1.73	-3.3	2.7	550	3.25	14.7π/σ
	C_2H_3-Br	1.89	-3.2	2.4	450	2.79	13.7σ
	* C_2H_3-I	2.09	-2.5	2.3	410	2.68	12.9σ
Assumption	C_2H_3-Br	1.95	-2.9	2.7	480	2.80	13.5σ
Assumption and PS data	* C_2H_3-Br	1.95	-2.8	2.5	460	2.97	13.6σ
Assumption	* C_2H_3-F	1.39	-3.8	3.2	700	4.20	15.0π
Experiment	C_2H_3-F	1.348†	-4.4	5.6	1100	1.43	10.37
	C_2H_3-Cl	1.736	-3.4	3.4	650	1.42	10.00
	C_2H_3-Br	1.891	-2.8	2.8	560	1.42	9.80
	C_2H_3-I	2.089	-2.5	2.3	500	1.27	9.33
	Ref.	(56)	(57)#	(66)#	(58)#	(59)	(60)

*Best results for C^{σ} = 2p.

#Average bond energies, force constants, and frequencies.

†Ref. (61).

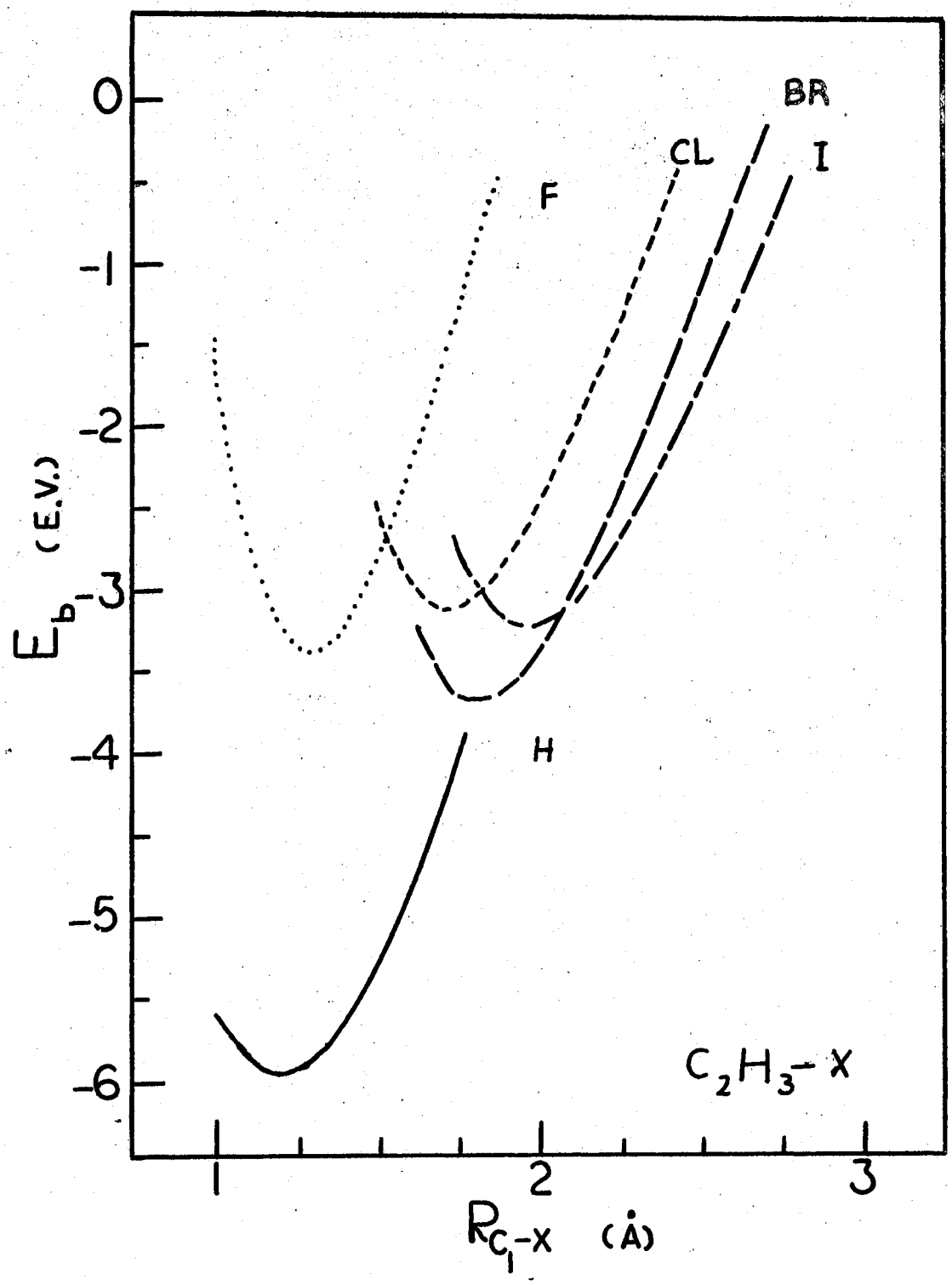

Figure 5. 10-10 Binding Curves for the C-X Bond in Haloethene With a 2tr Carbon Sigma Orbital

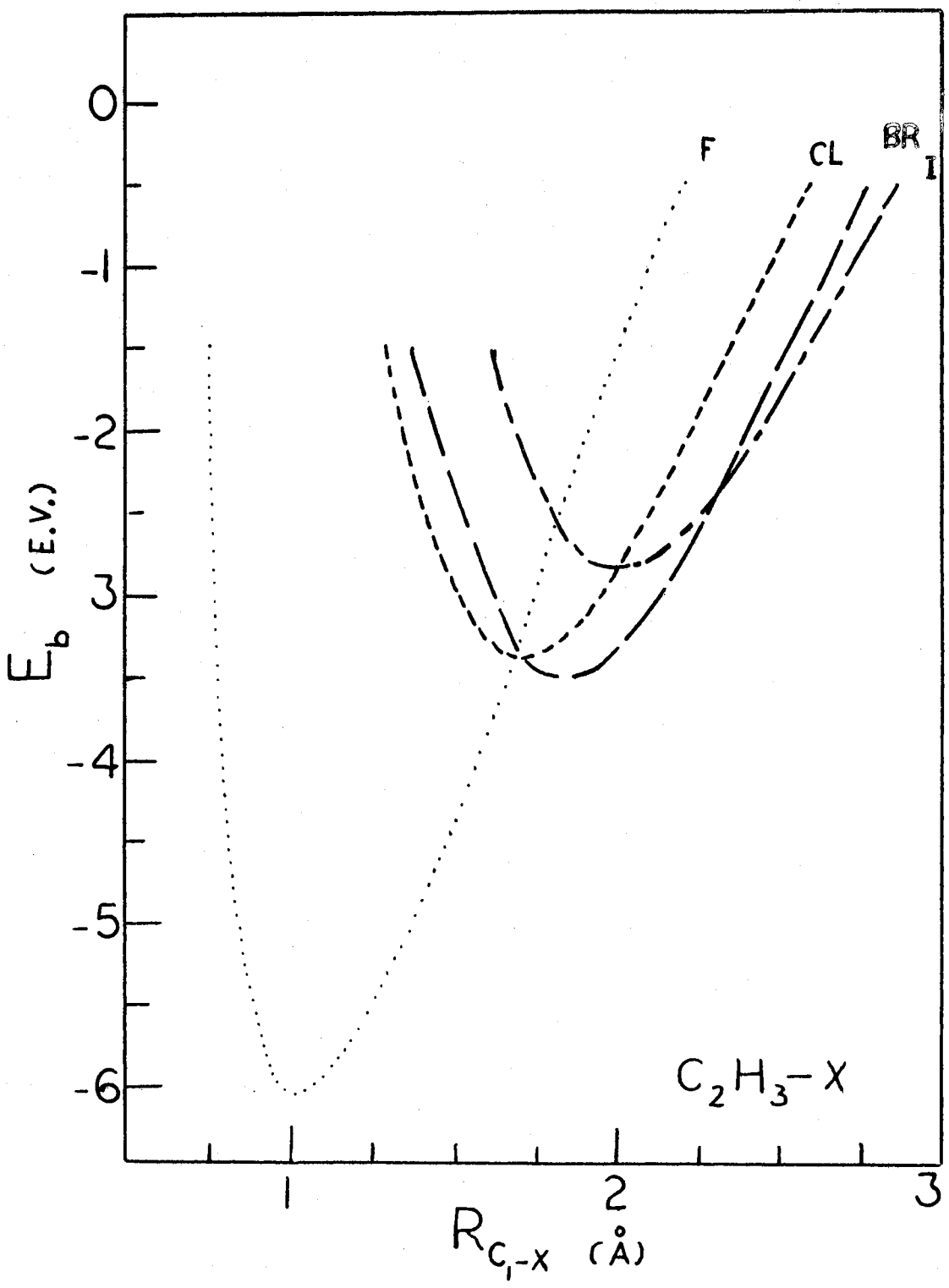

Figure 6. 10-10 Binding Curves for the C-X Bond in Haloethene With a 2p Carbon Sigma Orbital

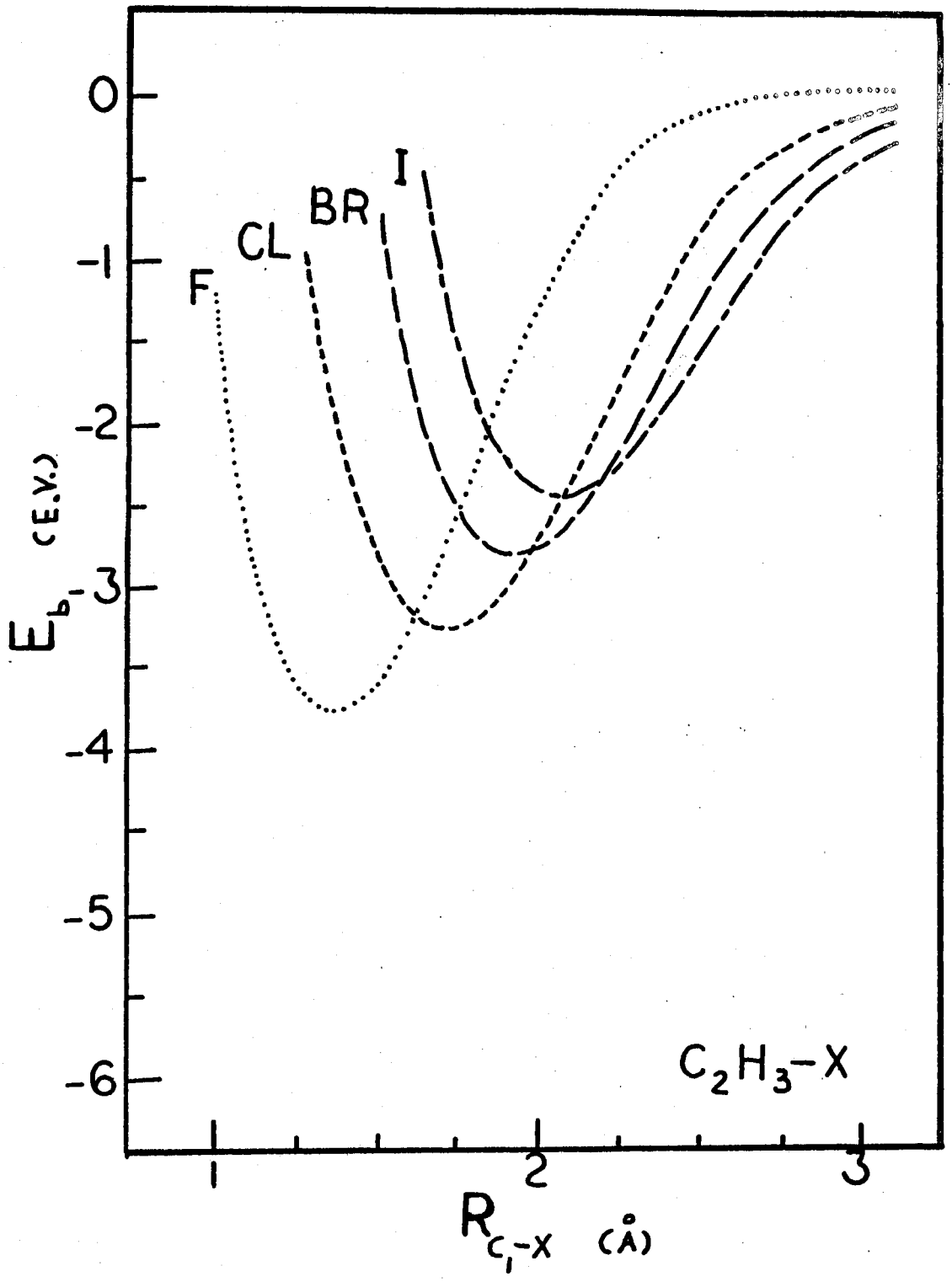

Figure 7. Best Binding Curves for the Haloethene C-X Bonds With a 2p Carbon Sigma Orbital

constants, stretching frequencies, and ionization potentials. The bond lengths are quantitatively predicted. The binding energies and frequencies are within 25-50% of the characteristic experimental values. However, the model molecular dipole moment is far off experiment, being a factor of 4 to 5 too low in the 2tr case and 2-3 too large in the 2p case. The dipole correction $\Delta\mu$ in the 2p case for C_2H_3F with $R_{CF} = 1.25\text{Å}$ is 0.043 Debyes along the direction F to C_1, or less than 1% of the computed molecular moment.

For computations on C_2H-X and C_6H_5-X the core repulsion parameters and bromine data described above as "best" are used along with a 2p carbon sigma AO, unless stated otherwise. The 10-10 core repulsion parameters and HJ data are used with 2tr.

Haloethynes

The haloethynes are computed with the C-C bond length and the CCX bond angle fixed at their respective experimental values, 1.21Å and 180°.[56,61] Example C_2HF wave functions for $R_{CF} = 1.25\text{Å}$ are displayed in Table XII for a 2p and a 2tr carbon sigma AO. The molecular orbital coefficients and energies are similar to those for the C_2H_3F computation. Table XIII shows the predicted bond and molecular properties. The results are qualitatively correct except for the dipole moments and C_2H-Br force constant. The bond length predictions for C_2H-F correctly decreases from the C_2H_3-F case. However, the C_2H-Cl and C_2H-Br bond lengths increase contrary to experiment. The C-X bond energies increase in magnitude from the haloethene case, in apparent agreement with a reported value of -4.94 e.V. for C_2H-F[61] compared to an average energy of -4.4 e.V. for C_2H_3-F[57]. The highest occupied molecular orbital energy I_m

TABLE XII

C_2HF MOLECULAR ORBITAL COEFFICIENTS AND ENERGIES AT $R_{CF} = 1.25\text{Å}$

Carbon Sigma Orbital	Atomic Orbital† Atom (nℓm)	Molecular Orbital* 1	2	3	4	5	6
2p	C_1(21-1)	1.0194	0.0	0.2918	0.0	0.0	0.0
	C_2(21-1)	-0.6140	0.0	0.8644	0.0	0.0	0.0
	C_1(211)	0.0	1.0194	0.0	0.2918	0.0	0.0
	C_2(211)	0.0	-0.6140	0.0	0.8644	0.0	0.0
	C_1(210)	0.0	0.0	0.0	0.0	1.0306	0.1466
	F(210)	0.0	0.0	0.0	0.0	-0.4271	0.9493
	ε_m(e.V.)	5.60	5.60	-18.55	-18.55	3.88	-23.18
2tr	C_1(21-1)	0.9571	0.0	0.4563	0.0	0.0	0.0
	C_2(21-1)	-0.7485	0.0	0.7510	0.0	0.0	0.0
	C_1(211)	0.0	0.9571	0.0	0.4563	0.0	0.0
	C_2(211)	0.0	-0.7485	0.0	0.7510	0.0	0.0
	C_1(200&210)	0.0	0.0	0.0	0.0	1.0029	0.3852
	F(210)	0.0	0.0	0.0	0.0	-0.7250	0.7928
	ε_m(e.V.)	5.34	5.34	-16.73	-16.73	2.07	-22.26

*Underlined MO's are occupied.

†See Figure 1 for a clarification of the subscripts.

TABLE XIII

RESULTS FOR THE HALOETHYNES

Method	Molecule	R_e^{CX} (Å)	E_b^{CX} (e.V.)	K^{CX} (md/A)	ν^{CX} (cm^{-1})	μ (D)	I_m (e.V.)
2tr Carbon Sigma AO							
10-10	C_2H-F	1.19	-5.0	3.7	760	.61	17.0π
2p Carbon Sigma AO							
Assumption	C_2H-F	1.33	-5.7	3.8	770	1.80	18.5π
5-5	C_2H-Cl	1.75	-4.9	3.2	610	.56	16.3σ
Assumption plus PS data	C_2H-Br	1.98	-4.4	3.4	530	1.12	14.6σ
5-5	C_2H-I	2.12	-4.0	3.0	490	1.24	14.0σ
Experiment							
	C_2H-F	1.279†	-4.94	8.8		.75	
	C_2H-Cl	1.632		5.4	756	.44	
	C_2H-Br	1.80		4.6	618	0	
	C_2H-I						
	Ref.	(56)	(61)	(62)	(63)	(59)	

†Ref. (61).

decreases from C_2HF to C_2HI, as expected from a consideration of electronegativity variations through the series.

The best binding curves for C_2H-F, C_2H-Cl, C_2H-Br, and C_2H-I are shown in Figure 8. They smoothly approach the limit $C_2H\cdot + X\cdot$, the energy of which is taken as zero.

The variation of the charge on the halogen atom with distance is shown in Table XIV. Again, the results are much the same as in the haloethene series. However, the occurrence of local minima at about 2.25, 2.50, 2.50, and 2.75 Å for C_2HF, C_2HCl, C_2HBr, and C_2HI, respectively, indicate a small burst of charge transfer at long range. Whether this is another antifact of the current model or physical reality will be an interesting problem to resolve as future model developments beyond the present study are explored. The equilibrium net atom charges and partial overlap populations are shown in Table XV. Using the POP as an index of bond strength, the C-X bonds become stronger through the halogen series, contrary to the computed and experimental decrease in binding energy. POP values apparently may be as indices of bond strength only for the same bond in different environments. The magnitude of the net charge transfer decreases.

Halobenzenes

The experimental geometries of the halobenzenes have, within their accuracy, 1.400Å for all of the equilibrium C-C bond lengths and 120° for all of the bond angles[56]. These values are assumed for the halobenzene computations.

Sample fluorobenzene wave functions are displayed in Table XVI. Computed results for the equilibrium properties are given in Table XVII.

TABLE XIV

VARIATION WITH DISTANCE OF THE NET ATOM CHARGE

ON THE HALOGEN ATOM IN THE HALOETHYNES

R_o (Å)	Q_X for C_2H-X			
	F	Cl	Br	I
0.75	-1.005			
1.00	- .995			
1.25	- .880	-.944		
1.50	- .763	-.694	-0.739	-.801
1.75	- .716	-.505	-0.462	-.459
2.00	- .717	-.446	-0.367	-.321
2.25	- .734	-.445	-0.352	-.287
2.50	- .142	-.468	-0.367	-.289
2.75	- .036	-.270	-0.362	-.306
3.00	- .009	-.101	-0.168	-.207
3.25		-.036	-0.066	-.096
3.50		-.012	-0.024	-.041
3.75				-.016

TABLE XV

HALOETHYNE EQUILIBRIUM NET ATOM CHARGES AND PARTIAL OVERLAP POPULATIONS WITH A 2P CARBON SIGMA ORBITAL

Molecule	Q			POP	
	C_1	C_2	X	$C_1(211)-C_2(211)$	C_1-X
C_2HF	2.076	-1.265	-.811	.357	.174
C_2HCl	1.139	-0.634	-.505	.465	.406
C_2HBr	0.792	-0.419	-.373	.484	.439
C_2HI	0.623	-0.318	-.305	.490	.439

TABLE XVI

C_6H_5F MOLECULAR ORBITAL COEFFICIENTS AND ENERGIES AT $R_{CF} = 1.25\text{Å}$

Carbon Sigma Orbital	Atomic Orbital Atom (nℓm)	Molecular Orbital* 1	2	3	4	5	6	7	8
2p	C_1(211)	0.9896	0.3736	0.0	-0.0380	0.0	0.1109	0.0	0.0
	C_2(211)	-0.3826	0.0677	-0.2222	-0.1862	0.7065	0.6314	0.0	0.0
	C_3(211)	0.2971	-0.6963	0.7390	0.0925	0.0482	0.0507	0.0	0.0
	C_4(211)	-0.1726	0.4590	0.0	0.9279	0.0	0.1766	0.0	0.0
	C_5(211)	0.2971	-0.6963	-0.7390	0.0925	-0.0482	0.0507	0.0	0.0
	C_6(211)	-0.3826	0.0677	0.2222	-0.1862	-0.7065	0.6314	0.0	0.0
	C_1(210)	0.0	0.0	0.0	0.0	0.0	0.0	1.0292	0.1561
	F(210)	0.0	0.0	0.0	<u>0.0</u>	<u>0.0</u>	<u>0.0</u>	-0.4358	<u>0.9453</u>
	ε_m(e.V.)	5.76	2.58	1.42	<u>-15.11</u>	<u>-16.61</u>	<u>-17.62</u>	5.00	<u>-18.72</u>
2tr	C_1(211)	0.8905	0.5547	0.0	-0.0706	0.0	0.1644	0.0	0.0
	C_2(211)	-0.4234	-0.0230	-0.2369	-0.2286	0.7017	0.5935	0.0	0.0
	C_3(211)	0.4248	-0.6259	0.7378	0.0875	0.0636	0.0665	0.0	0.0
	C_4(211)	-0.2540	0.4222	0.0	0.9106	0.0	0.2463	0.0	0.0
	C_5(211)	0.4248	-0.6259	-0.7378	0.0875	-0.0636	0.0665	0.0	0.0
	C_6(211)	-0.4234	-0.0230	0.2369	-0.2286	-0.7017	0.5935	0.0	0.0
	C_1(200&210)	0.0	0.0	0.0	0.0	0.0	0.0	1.0185	0.3418
	F(210)	0.0	0.0	0.0	<u>0.0</u>	<u>0.0</u>	<u>0.0</u>	-0.6904	<u>0.8231</u>
	ε_m(e.V.)	5.35	2.72	1.91	<u>-14.53</u>	<u>-15.18</u>	<u>-16.54</u>	2.20	<u>-20.14</u>

*Underlined MO's are occupied.

†See Figure 2 for a clarification of the subscripts.

TABLE XVII

HALOBENZENES

Method	Molecule	R_e^{cx} (Å)	E_b^{cx} (e.V.)	K^{cx} (md/Å)	ν^{cx} (cm^{-1})	μ (D)	I_m (e.V.)
Carbon Sigma AO = 2p							
Assumption	* C_6H_5F	1.26	-6.54	4.7	730	5.51	15.1π
5-5	* C_6H_5Cl	1.63	-5.28	2.7	430	6.29	15.0σ
Assumption and PS Data	* C_6H_5Br	1.89	-4.42	2.5	330	6.47	12.4σ
5-5	* C_6H_5I	2.03	-3.84	2.1	270	6.46	12.6σ
Carbon Sigma AO = 2tr							
10-10	C_6H_5F	1.19	-4.98	4.5	710	3.88	14.6π
	C_6H_5Cl	1.69	-3.51	3.4	490	2.70	14.0π
	C_6H_5Br	1.79	-3.93	3.2	370	2.70	12.2π
	C_6H_5I	1.94	-3.47	2.6	300	2.95	12.1π
Experiment							
	C_6H_5F	1.305	-4.6	5.6	1100	1.66	9.67
	C_6H_5Cl	1.69	-3.5	3.4	650	1.70	9.42
	C_6H_5Br	1.86	-2.94	2.8	560	1.70	10.49
	C_6H_5I	2.08	-2.5	2.3	500	1.71	9.10
	Ref.	(56)	(61)	(66)#	(58)	(59)	(60)

*Best results.

#Average bond force constants.

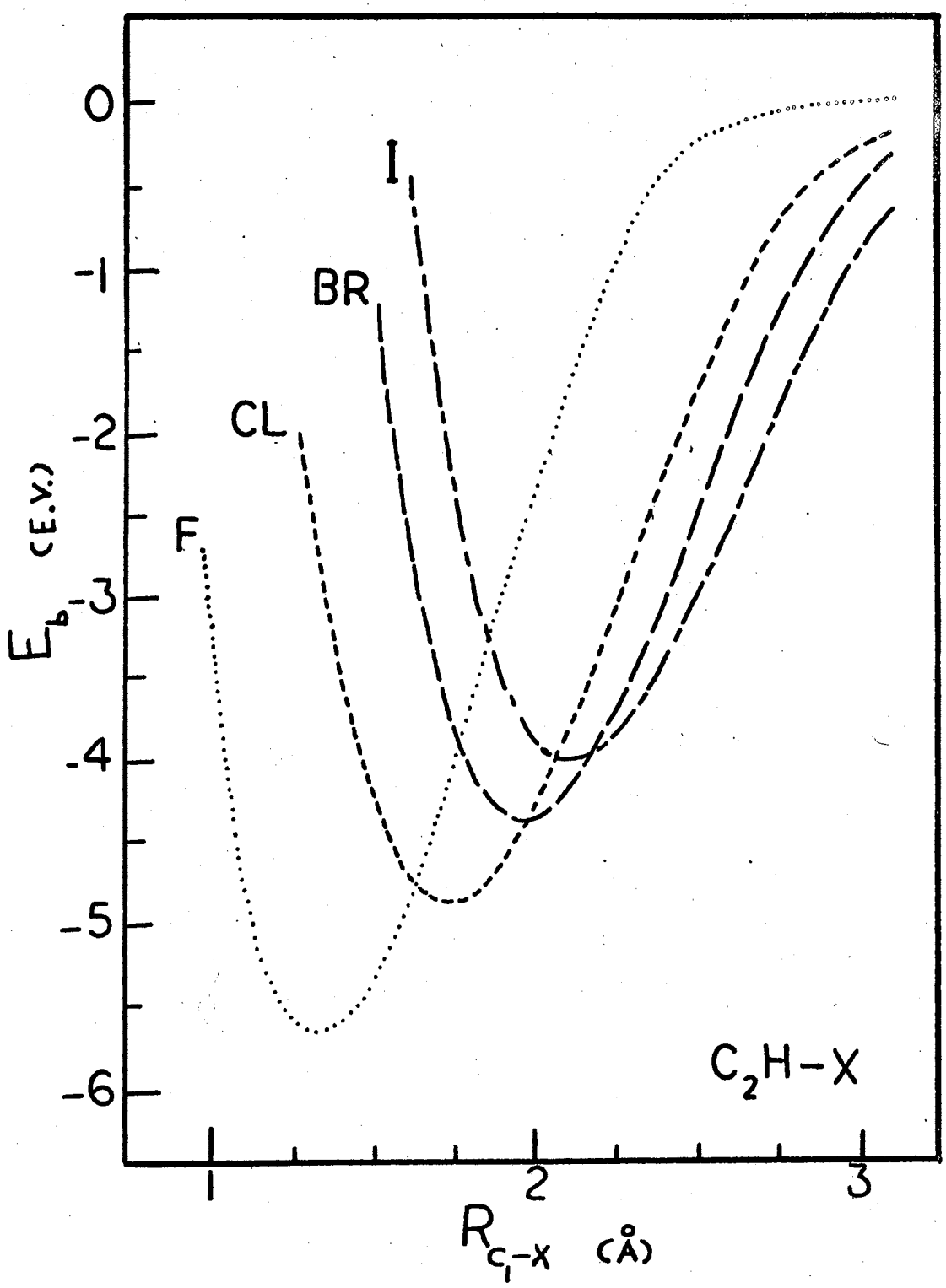

Figure 8. Haloethyne C-X Binding Curves

The 10-10 2tr binding curves are shown in Figure 9 and the best results with a 2p in Figure 10. The equilibrium Q and POP values are displayed in Table XVIII.

The halobenzene results are very similar to those for the haloethenes. It will also be noted that through the halogen series F, Cl, Br, I the C_6H_5-X bond lengths decrease and the dipole moments increase from the C_2H_3-X results. These variations are in agreement with experiment. In accordance with general expectations, the absolute values the binding energies increase from C_2H_3-X to C_6H_5-X. The large charge oscillation about the ring found for the phenyl radical persists in the halobenzene wave function (Table XVIII).

The ionization potentials are about 2-5 e.V. too high. The values for fluorbenzene, 15.1 and 14.6 e.V., compare with the 13.3 e.V. result of a recent all-valence electron computation by Bloor and Bleen[64].

The halobenzene charge distributions, dipole moments and ionization potentials are in qualitation agreement with the results of Mataga-Pariser-Parr-Pople computations by Knowlten and Carper[65]. They report a charge oscillation about the benzene ring of amplitude about 0.3.

Table XIX displays the C-F binding energy variation with the CCF angle in fluorobenzene. As may be seen, the model contains enough information about the molecule to correctly predict the correct bond angle and also a symmetric angular potential. The bonding force constant is of about the right size[66]. It is common knowledge in semiempirical molecular theory that angular geometry is the easiest molecular property to predict[67]. The present result indicates successful fulfillment of a minimum criterion of model acceptability.

The striking aspect of the present study is that bond lengths are

TABLE XVIII

HALOBENZENE EQUILIBRIUM NET ATOM CHARGES

AND PARTIAL OVERLAP POPULATIONS[†]

Quantity		Molecule			
		C_6F	C_6CL	C_6BR	C_6I
2tr Carbon Sigma AO; 10-10 Core Repulsion Parameters					
Q	C_1	1.45	0.97	-0.99	-0.98
	C_2	-0.88	-0.81	0.82	0.82
	C_3	0.89	0.87	-0.88	-0.88
	C_4	-0.87	-0.86	0.85	0.85
	X	-0.61	-0.26	+0.21	0.24
POP	C_1-C_2	0.10	0.14	0.15	0.15
	C_2-C_3	0.06	0.08	0.07	0.07
	C_3-C_4	0.09	0.10	0.10	0.10
	C_1-X	0.40	0.60	0.66	0.63
2p Carbon Sigma AO; Best Core Repulsion Parameters					
Q	C_1	1.76	1.51	1.44	1.37
	C_2	-0.92	-0.88	-0.86	-0.85
	C_3	0.90	0.90	0.89	0.89
	C_4	-0.87	-0.86	-0.86	-0.86
	X	-0.87	-0.70	-0.63	0.59
POP	C_1-C_2	0.08	0.11	0.12	0.13
	C_2-C_3	0.05	0.05	0.05	0.05
	C_3-C_4	0.09	0.10	0.10	0.10
	C_1-X	0.16	0.29	0.35	0.37

[†]See Figure 2 for clarification of the subscripts.

TABLE XIX

IN-PLANE VARIATION OF THE C-C-F ANGLE IN FLUOROBENZENE

R_{CF} = 1.305 Å	C^{σ} = 2tr	10-10 Core Repulsion

CCF Angle (Degrees)	E_b (e.V.)	Equilibrium Values	
110	-4.748	CCF Angle	120^{o}
115	-4.789	E_b	-4.803 e.V.
120	-4.803	K	1.13×10^{-3} e.V./deg.^{2}
125	-4.789	$K/R_{CC}R_{CF}$	0.32×10^{5} dyne/cm.
130	-4.748		

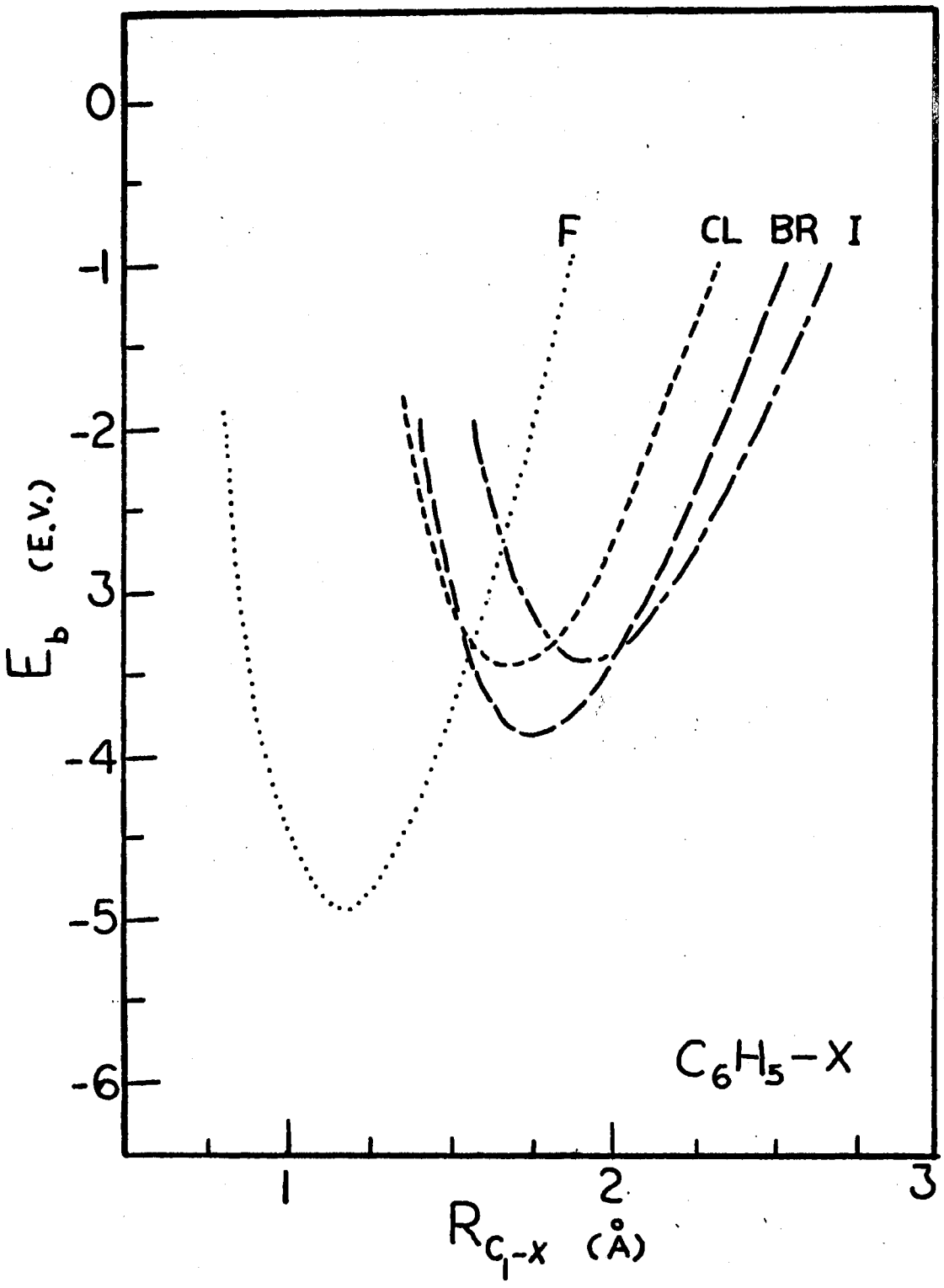

Figure 9. 10-10 Binding Curves for the Halobenzene C-X Bond With a 2tr Carbon Sigma Orbital

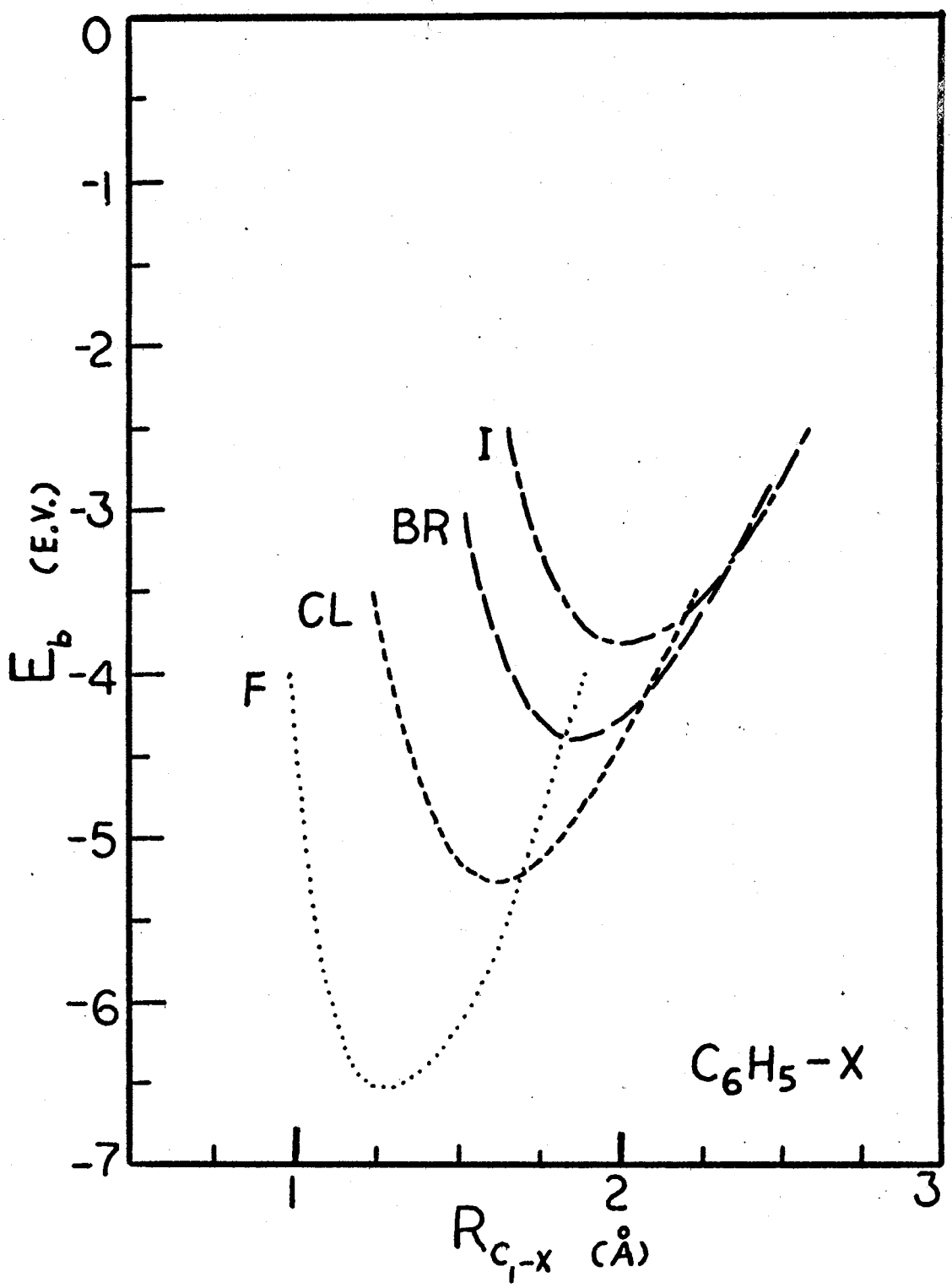

Figure 10. Best Binding Curves for the Halobenzene C-X Bond With a 2p Carbon Sigma Orbital

so well predicted. Uncalibrated semiempirical models are very seldom found able in this aspect of geometry prediction.

Ethene, Ethyne, and the Hydrogen Molecule

Trial results for ethene are shown in Table XX. The model is credible only for C_2H_3-H with a 10-10 core repulsion and a 2tr carbon sigma AO. This binding curve is shown in Figure 5. Computations for C_2H-H fail even to show a minimum for C-H separation as small as 0.25Å. Apparently hydrogen must be considered to have a core repulsion "correction" even though there appears to be no core penetration adjustment to be made. Otherwise, the C-H bond in ethyne is not properly recognized by the current development of the model. A similar problem arises with application to the diatomic H_2: core repulsion does not increase rapidly enough with decreasing atom separation to produce a credible bond length and binding energy from the rapidly decreasing electronic energy curves.

The H-H and C-H bond trials not withstanding, the model does a credible job of predicting and correlating several molecular properties from the limited input of atomic data. The information content of the pi and substituted bond sigma-electrons is seen to be considerable.

TABLE XX

ETHENE

Quantity	Value		Expmt.	Ref.
	C^{σ} = 2tr	C^{σ} = 2p		
Core Repulsion Parameters ($\AA^{-1}$)				
Carbon	10-10	10-10		
Hydrogen	100	100		
C_2H_3-H Bond Properties				
R_e^{CH} ($\AA$)	1.19	0.44	1.071	(56)
E_b^{CH} (e.V.)	-6.0	-23.	-4.3	(57)
K (md/$\AA$)	3.2	——	5.1	(66)
ν (cm^{-1})	2400	>10,000	2900	(58)
μ (D)	0.86	5.69	0	(59)
I_m(e.V.)	12.4	13.0	11.51	(60)
Net Atomic Charge Q				
C_1	-0.28	2.11		
C_2	0.12	-1.01		
H	0.16	-1.10		
Partial Overlap Population POP				
C_1-C_2(π)	0.42	-0.04		
C_1-H(σ)	0.77	-0.45		

CHAPTER IV

CONSIDERATION OF MOLECULES WITH FOUR ATOM SIGMA ELECTRON SYSTEMS

Results presented in Chapters II and III show the merit of selected valence-electron models of diatomics and planar pi-moiety compounds. The ability of such models to describe di-substituted and small sigma-electron systems of more than two centers is also of interest. As noted in Chapter I, such models of three atom hydrogen-bonding systems have been tested and with considerable success[24-26]. In this chapter, the four atom H_2I_2 system is examined at two postulated saddle point configurations and the three dichloroethene isomers are considered with regard to properties determined by the C-Cl sigma- and C-C pi-bonding electrons.

Application of the Model to the Dichloroethenes

The $C_2H_2Cl_2$ computations are carried out with a 2tr carbon sigma orbital and the 10-10 core repulsion parameters for the determination of bond properties. Results are presented for 1,1-$C_2H_2Cl_2$, cis-1,2-$C_2H_2Cl_2$ and trans-1,2-$C_2H_2Cl_2$. The requisite radical computations are presented in Table XXI.

For each isomer the symmetric stretching motions are investigated by varying both C-Cl bonds in unison along their experimental equilibrium direction. Single C-Cl bond strecthing force constants are evaluated by

TABLE XXI

ETHENE DI-SIGMA RADICALS

Property	cis- and trans-1,2-di-radical	1,1-diradical
E(e.V.)	-125.19	-125.66
Q_1, Q_2	0,0	0,0
POP_{12}	.403	.403
I_m(e.V.)	13.2	13.2

varying one C-Cl bond with the other fixed at the computed equilibrium distance. A sample wave function for 1,1-$C_2H_2Cl_2$ is displayed in Table XXII. The summarized results for the three isomers are presented in Table XXIII. In these computations, R_{CC} = 1.38Å, which is an assigned value for $C_2H_2Cl_2$.[56]

From the results shown in Table XXIII it can be seen that the model is capable of good bond length predictions for multisubstituted molecules. The C-Cl bond energies are reasonable for the cis and trans isomers, but the 1,1-$C_2H_2Cl_2$ binding energy is too large in magnitude. Based on the relative energies of the C-Br bond in 1,2-$C_2H_2Br_2$(-2.86 e.V.) and 1,1-$C_2H_2Br_2$(-2.73 e.V.)[56], it would be expected that the magnitude of the C-Cl bond energy in 1,1-$C_2H_2Cl_2$ is less than in 1,2-$C_2H_2Cl_2$. The model account of Cl-Cl interaction seems to be the most likely source of the flaw since the two chlorine atoms in 1,1-$C_2H_2Cl_2$ are much closer together than in the other two isomers.

The symmetric C-Cl stretching motions for 1,1-$C_2H_2Cl_2$ (900 cm^{-1}) and trans-1,2-$C_2H_2Cl_2$ (800 cm^{-1}) are roughly comparable to the normal modes (820 or 844 cm^{-1} for trans-1,2-$C_2H_2Cl_2$)[58]. The symmetric cis-1,2-$C_2H_2Cl_2$ stretching motion (800 cm^{-1}) is also comparable to the experimental mode primarily determined by the simultaneous C-Cl stretch (857 cm^{-1})[58]. The single C-Cl bond stretching force constants (4.44, 3.58, and 3.57 md/Å for 1,1-$C_2H_2Cl_2$, cis-1,2-$C_2H_2Cl_2$, and trans-1,2-$C_2H_2Cl_2$, respectively) are greater than the value obtained for C_2H_3Cl (3.4 for C^{σ} = tr) and the characteristic value (3.4)[66].

As for molecular dipole moments, the model correctly predicts that the moment of cis-1,2-$C_2H_2Cl_2$ is about twice that of 1,1-$C_2H_2Cl_2$ and that trans-1,2-$C_2H_2Cl_2$ has no net molecular charge displacement. As

TABLE XXII

1,1-DI-CHLOROETHENE MOLECULAR ORBITAL COEFFICIENTS AT R_{C-CL} = 1.75 Å AND <CL-C-CL = 122°

Atomic Orbital Atom (nℓm)	Molecular Orbital*					
	1	2	3	4	5	6
C_1(211)	.8196	.6297	0.0	0.0	0.0	0.0
C_2(211)	- .8196	.6297	0.0	0.0	0.0	0.0
C_2(2tr)	0.0	0.0	-0.7029	-0.6644	0.3892	- .4200
C_2(2tr)	0.0	0.0	-0.7029	0.6644	-0.3892	- .4200
Cl_3(310)†	0.0	0.0	0.6883	0.6508	0.4565	- .3952
Cl_4(310)#	0.0	0.0	0.6883	-0.6508	-0.4565	- .3952
ε_m(e.V.)	3.20	-13.51	5.45	4.68	-16.70	-18.13

*Underlined MO's are occupied.

†Cl_3 bonded to C_1.

#Cl_4 bonded to C_2.

TABLE XXIII

DICHLOROETHENE

Molecule	Varied Bond(s)	R_e^{cx} (Å)	E_b^{cx} (e.V.)	ν (cm^{-1})	μ (D)	I_m (e.V.)
$1,1\text{-}C_2H_2Cl_2$	Both C-Cl,					
<Cl-C-Cl = 122°	symmetrically	1.75	-5.98	900	.25	13.5
	One C-Cl, other = 1.75Å	1.75	-5.98	580	.25	13.5
	Experiment	1.69[56]	3.4*		1.25[59]	9.8[60]
$cis\text{-}1,2\text{-}C_2H_2Cl_2$	Both C-Cl,					
<Cl-C-Cl = 123.5	symmetrically	1.71	-2.74	800	.53	13.5
	One C-Cl, other = 1.71Å	1.71	-2.74	520	.52	13.5
	Experiment	1.67[56]	3.4*	857[58]	2.95[59]	9.7[60]
$trans\text{-}1,2\text{-}C_2H_2Cl$	Both C-Cl,					
<Cl-C-Cl = 122.5	symmetrically	1.71	-2.78	800	0.00	13.4
	One C-Cl, other = 1.71Å	1.71	-2.78	520	.01	13.4
	Experiment	1.69[56]	3.4*	820,844[58]	0[59]	10.0[60]

*Average bond energy. Ref. (57).

found in Chapter III, use of $C^{\sigma} = 2tr$ produces dipole moments which are about a factor of five too small.

The highest occupied molecular orbital energies I_m do not correlate well with the molecular ionization potentials. The model does correctly predict a closely grouped set of values of I_m for the three isomers.

Variation of the Cl-C-Cl angle in 1,1-$C_2H_2Cl_2$ produces a computed minimum energy angle of 129° for $R_{C-Cl} = 1.75\text{Å}$. The bonding energy with respect to ($CH_2C: + 2Cl\cdot$) is plotted against the Cl-C-Cl angle in Figure 11. The experimental values are 122° and 1.69Å.[56] Wilson, Decius and Cross[66] quote an approximate Cl-C-Cl bending force constant of $K/R^2_{C-CL} = .33 \times 10^5$ dyne/cm from a valence bond force field treatment of CCl_4. This compares with a computed value of $.11 \times 10^5$ dynes/cm in 1,1-$C_2H_2Cl_2$ with $R_{C-CL} = 1.750\text{Å}$. Thus a reasonable account of the three center angle is given by an explicit consideration of only the bonding valence electrons.

The results for $C_2H_2Cl_2$ show that the model is reliable in predicting geometry and dipole moment variations of multisubstituted molecule. The performance on binding energies among the isomers of dichloroethene is good for large Cl-Cl separations. The model is not capable of predicting highest occupied molecular orbital energies in quantitative agreement with experimental ionization potentials of multisubstituted ethene. However, the present tests show that the uncalibrated initial form of the model developed in the present study is capable of describing some of multisubstituted molecular properties which may be considered to be primarily determined by a selected few valence electrons.

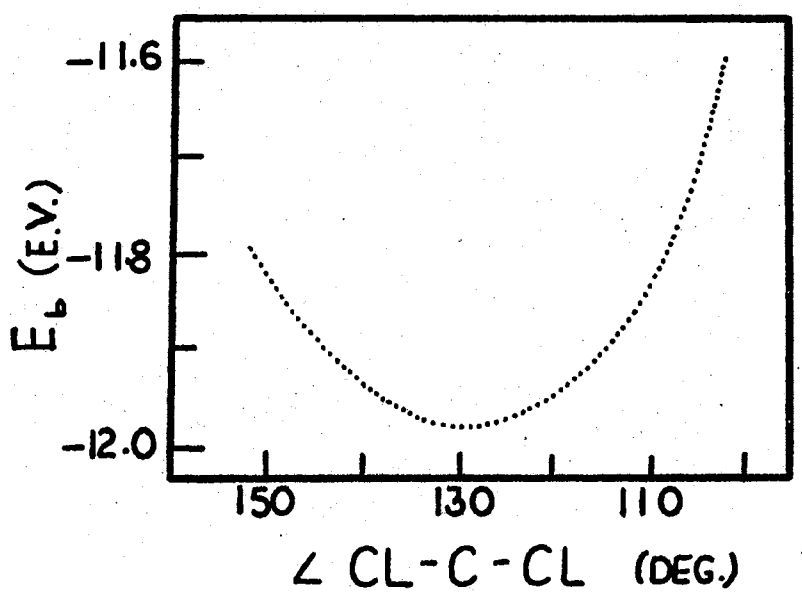

Figure 11. Binding Energy of the Two C-CL Bonds in 1,1-$C_2H_2CL_2$ Versus the CL-C-CL Angle at R_{C-CL} = 1.75 Å

H_2I_2 Saddle Points

The four atom H_2I_2 system is examined at the regular planar trapezoidal and symmetric linear saddle points reported by Raff, Stivers, Porter, Thompson, and Sims[68]. The model they used is described in Chapter I. The present model is described in Chapter II.

The geometry of the trapezoidal configuration is specified by the HI-HI (5.569 a.u.) and HH-II (3.272 a.u.) center of mass distances with the assumption that the I-I separation is equal to the H-H separation plus the difference between the equilibrium H-H and I-I bond lengths[68]. The linear saddle point is specified by 1.51 a.u. for H-H and 9.97 a.u. for I-I[68].

The wave functions obtained are displayed in Table XXIV. The molecular orbital symmetries are in accord with expectations. Again it is seen that the unrestricted wave function is equivalent to a restricted one for atoms in close proximity.

The saddle point energies are computed using two methods to calculate the core repulsion. One is the use of the core repulsion described in Chapter II with the 10-10 parameters. The other is a summation of the assigned core charge repulsions

$$E_{cr} = \sum_{a<b} Z_a^c Z_b^c / R_{ab} .$$

Saddle-point stabilization energies with respect to the neutral atoms H + H + I + I and with respect to the homonuclear molecules H_2+I_2 are shown in Table XXV. The molecular energies of H_2 (-33.83) and of I_2 (-25.26 e.V.) are computed at their respective equilibrium separations[57].

TABLE XXIV

H_2I_2 SADDLE POINT WAVE FUNCTIONS

Spin	Atomic Orbital† Atom (nℓm)	Trapezoidal Molecular Spin Orbital* 1	2	3	4	Linear Molecular Spin Orbital* 1	2	3	4
α	I_1(510)	0.3469	0.7391	0.6891	-0.1571	0.3176	0.7301	0.6844	-0.1133
	H_2(100)	-1.1706	-0.3654	0.1531	-0.4943	-1.4239	-0.2481	0.1197	-0.5068
	H_3(100)	1.1706	-0.3654	-0.1531	-0.4943	1.4239	-0.2481	-0.1197	-0.5068
	I_4(510)	-0.3469	0.7391	-0.6891	-0.1571	-0.3176	0.7301	-0.6844	-0.1133
	ε_m(e.V.)	11.34	-3.50	-10.86	-17.18	19.21	-5.50	-9.88	-18.26
β	I_1(510)	0.3469	0.7391	0.6891	-0.1572	0.3176	0.7301	0.6844	-0.1133
	H_2(100)	-1.1706	-0.3654	0.1531	-0.4943	-1.4239	-0.2481	0.1197	-0.5068
	H_3(100)	1.1706	-0.3654	-0.1531	-0.4943	1.4239	-0.2481	-0.1197	-0.5068
	I_4(510)	-0.3469	0.7391	-0.6891	-0.1572	-0.3176	0.7301	-0.6844	-0.1133
	ε_m(e.V.)	11.34	-3.50	-10.86	-17.18	19.21	-5.50	-9.88	-18.26

*Underlined MSO's are occupied.

†See Figure 3 for clarification of the subscripts.

TABLE XXV

H_2I_2 ENERGIES AT THE LINEAR AND TRAPEZOIDAL SADDLE POINTS IN E.V.

Surface	Exp.	Core Repulsion		Raff, et. al.	Minn and Hanratty
		$Z_a^*Z_b^*/R_{ab}$	$Z_a^cZ_b^c/R_{ab}$		
	(33)	$Z_a^* = Z_a^c + (Z_a^n - Z_a^c)\ \mathrm{Exp}(-D_a R_{ab})$		(27)	(69)
Linear					
E, ref = atoms		-3.74	-3.93		
E, ref = $H_2 + I_2$	1.77	2.80	2.62	1.98	2.5,3.5
Trapezoidal					
E, ref = atoms		-3.63	-4.19		
E, ref = $H_2 + I_2$	1.77	2.92	2.35	1.82	3.7,5.3
$E_L - E_T$		-0.12	0.27	.16	-1.2,-1.8

From the results presented in Table XXV it is apparent that the method of computing core repulsion determines the relative stability of the linear and trapezoidal saddle point. The $Z_a^c Z_b^c/R_{ab}$ method predicts the trapezoidal configuration is lower in energy than the linear, in accordance with the results of Raff, et al.[68] The exponential method, which adds on iodine core penetration correction to $Z_a^c Z_b^c/R_{ab}$, predicts that the linear configuration is the more stable. Minn and Hanratty[69] found a linear configuration more stable than a trapezoidal in their recently reported valence bond computations on H_2I_2. However, the magnitude of their computed energy difference between the two configurations is much larger than either the present result or that of Raff, et al.[68] (Table XXV).

The model presented in Chapter II of this study is capable of predicting H_2-I_2 energies in reasonable accord with those published and of doing so without calibration to experimental data on H_2,I_2 and HI. However, the model description of the H-H interaction is not adequate. For example, the computed binding energy at R_e is -33.83-(-27.21) = -6.62 e.V., compared to the experimental value -3.83 e.V.[70] The faults cancel somewhat in the computation of the saddle point with respect to $H_2 + I_2$, but variation of H-H distance would produce non-physical results. As shown in Chapter III, the approximations of Chapter II do not lead to a reasonable binding curve for H_2. Better results should be obtainable by optimization of (1) core repulsion parameters for H and I and (2) an appropriate parameter in the electronic energy expression. Integral approximation expressions may also be varied. With such optimization, the model could be used to examine selected portions of the H_2-I_2 potential surface.

In summary, the results of this chapter indicate that selected valence electron models in unadjusted form have the capability of producing reasonable descriptions of sigma and sigma-pi coupled systems.

CHAPTER V

SOME EFFECTS OF VARIATION OF THE MODEL APPROXIMATIONS

Phenyl Charge Oscillation Problem

In the computations on the mono-substituted benzenes there occurred an extreme oscillation of charge about the ring. For progress on such molecules, the source of this model failure must be located and corrective alteration proposed. As a first step, computations on several pi-electron carbon ring and chain systems have been made. The net atom charges and electronic energy for each case examined are displayed in Table XXVI. A 2tr carbon sigma AO is used unless specified otherwise.

The extreme net charge variation about the ring in the mono-sigma phenyl radical is seen to be insensitive to the choice of a 2p in place of the 2tr. This is to be expected from the manner in which the sigma electron interacts through the integral approximations with the pi-electrons. But, if C_6 is rotated 90° out of the ring about C_5, the magnitude of the oscillation is smaller. A further reduction occurs if C_1 is rotated out 120° about C_2. These atom movements reduce the interactions of the doubly charged C_1 core.

On the other hand, if the VSIP and VSEA values for the pi-AO on C_1 are increased by 1 e.V., the oscillation suffers a sign change. The same effect is achieved by increasing the C_1(211) SZO orbital exponential from 1.625 to 1.800. Both of these modifications effectively increase

the electronegativity of the substituted carbon.

A computation for pi-only benzene gives neutral atoms. Also, a zig-zag chain with a sigma AO on one terminal carbon has only a small net charge on each atom. Similar results are obtained for a pi-electron-only carbon chain. A rectilinear chain, however, has a charge oscillation of the magnitude of the phenyl ring with C_6 moved.

Thus, the ring charge oscillation problem is a result of the use of a core charge of 2 with a close grouping of atoms. The one-center electron repulsion integrals are apparently not as effective in the determination of charge distribution as are the two-center integrals. The polarity of the oscillation depends upon the electronegativity of the substituted atom with respect to the others. The relative electronegativity depends in turn upon the choice of input atomic parameters.

There is one other method by which the model results may be altered. The integral approximation expressions may be varied. In particular, the Mataga and Nishimoto[70] expression $1/(R + r)$ may be used in place of the Pople[7] $1/R$ to evaluate the coulomb repulsion and core attraction integrals. For this modification Equations (7) and (6) are replaced, respectively, by Equation (70),

$$(pp|qq) \simeq 1/(R + r), \tag{70}$$

where p and q are on different atoms and

$$r = 2/((pp|pp + (qq|qq)),$$

and by Equation (71),

$$(pp/a) \cong 1/(R + r), \tag{71}$$

where r = 1/(qq/a) and p is not centered on atom a but q is. The results for the phenyl sigma radical are included in Table XXVI. The net atomic charges are much smaller than the Pople 1/R results. They are in fact of a magnitude characteristic of all valence electron computations on similar molecules reported recently by Pople and Gordon[71].

The unrestricted wave function computed for the Mataga-Nishimoto phenyl sigma radical does not have equivalent α and β MO's as does the Pople radical. This wave function characteristic is carried over in fluorobenzene when it is obtained by use of Equations (70) and (71). A sample C_6H_5F wave function is presented in Table XXVII. It may be compared with Table XVI, which presents the original results for fluorobenzene.

Variation of R_{CF} produces an electronic energy curve that decreases monotonically with R_{CF}. An attempt to compute a binding curve with the 5-5 core repulsion parameters produced an antibinding curve. Core repulsion must be optimized for the Mataga-Nishimoto approximation if it is to be used.

Sensitivity of the Diatomic Model to Its Component Quantities

It is apparent that the entire set of approximations made in the evaluation of the integrals and core repulsion must be examined. Optimization of the model will require determination of the parameters by calibration to experimental molecular data. The approximations developed in this study depend mostly upon atomic information in the description of bonds.

The first step in the optimization procedure is to determine how sensitive the computed quantities are to the various pieces of informa-

TABLE XXVI

NET ATOM CHARGES FOR SEVERAL PI SYSTEMS[†]

Pi-System	Net Atom Charge						E_e
	1	2	4	4	5	6	(e.V.)
Phenyl Sigma Radical*							
C^{σ} = 2tr	.72	- .79	.86	- .86	.86	- .79	-254.81
C^{σ} = 2p	.72	- .79	.86	- .86	.86	- .79	-249.08
C_6 rotated 90° out	.42	- .40	.66	- .65	.51	- .53	-235.63
C_6 rotated 90° and C_1 120° out	.25	- .24	.47	- .47	.45	- .47	-224.69
C_1^{π} VSIP and VSEA incr. in magnitude by 1 e.V.	- .79	.83	- .87	.86	- .87	.83	-256.48
$\zeta(C_1)$ = 1.800 instead of 1.625	- .72	.79	- .86	.85	- .86	.79	-254.91
Matago-Nishimoto approx.	.11	- .08	.03	- .004	.03	- .08	-230.50
Pi-only benzene	0.0	0.0	0.0	0.0	0.0	0.0	-185.76
Zig-zag chain, CCC <'s = 120°, sigma AO on one end	.002	.006	.092	- .092	.139	- .144	-222.02
Rectilinear chain, sigma AO on one end	.50	- .48	.77	- .77	.67	- .69	-215.01

*C^{σ} = 2tr unless stated otherwise.

†See Figure 2 for clarification of the subscripts.

TABLE XXVII

FLUOROBENZENE MOLECULAR SPIN ORBITALS AT R_{CF} = 1.25 Å WITH THE MATAGA-NISHIMOTO APPROXIMATION

Spin	Atomic Orbital† Atom (nℓm)	Molecular Spin Orbital* 1	2	3	4	5	6	7	8
α	C_1(211)	.5832	0.0	-0.7477	0.1972	0.0	0.4411	0.0	0.0
	C_2(211)	-0.4942	-0.3369	0.3033	0.1469	0.6595	0.4759	0.0	0.0
	C_3(211)	0.5934	0.7206	0.4220	-0.2076	0.1708	0.1047	0.0	0.0
	C_4(211)	-0.4546	0.0	-0.4617	-0.8302	0.0	0.1536	0.0	0.0
	C_5(211)	0.5934	-0.7206	0.4220	-0.2076	-0.1708	0.1047	0.0	0.0
	C_6(211)	-0.4942	0.3369	-0.3033	0.1469	-0.6595	0.4759	0.0	0.0
	C_1(210)	0.0	0.0	0.0	0.0	0.0	0.0	0.9581	0.4071
	F (210)	0.0	0.0	0.0	0.0	0.0	0.0	-0.6572	0.8073
	ε_m (e.V.)	-4.02	-7.21	-7.39	-17.63	-17.71	-20.45	-6.41	-21.75

TABLE XXVII (Continued)

Spin	Atomic Orbital† Atom (nℓm)	Molecular Spin Orbital* 1	2	3	4	5	6	7	8
β	C_1(211)	-0.5659	0.4332	0.0	0.0	0.4904	-0.6200	0.0	0.0
	C_2(211)	0.6125	-0.3457	-0.6930	-0.2612	0.0872	-0.2863	0.0	0.0
	C_3(211)	-0.4271	-0.2532	0.4182	-0.6112	-0.5212	-0.2571	0.0	0.0
	C_4(211)	0.5428	0.8638	0.0	0.0	-0.2881	-0.0944	0.0	0.0
	C_5(211)	-0.4271	-0.2532	-0.4182	0.6112	-0.5212	-0.2571	0.0	0.0
	C_6(211)	0.6125	-0.3457	0.6930	0.2612	0.0872	-0.2863	0.0	0.0
	C_1(210)	0.0	0.0	0.0	0.0	0.0	0.0	0.9581	0.4070
	F (210)	0.0	0.0	0.0	<u>0.0</u>	<u>0.0</u>	<u>0.0</u>	-0.6571	<u>0.8073</u>
	ε_m(e.V.)	-3.88	-6.80	-8.25	<u>-17.55</u>	<u>-17.63</u>	<u>-20.29</u>	-6.41	<u>-21.75</u>

*Underlined MSO's are occupied.

†See Figure 2 for clarification of the subscripts.

tion from which they are derived. Such a study should allow a more ready determination of the nature of alteration required in given cases to produce results more nearly in accordance with experiment.

As part of the examination of the selected valence electron model in this study, the sensitivity of the electronic energy E to its components is explored. The component quantities of the two-center two-electron model (see Chapter II) of hydrogen fluoride are altered systematically by small fractions of their value. The overlap integral S_{ab}, the two-center one-electron integral $H12_{pq}$, and the valence-state ionization potential of hydrogen $VSIP_H$ are varied over a wide range.

An unrestricted wave function is used. Because the molecular orbital form of the unrestricted function is complex for diatomics just inside of the equilibrium separation, the function is transformed to the equivalent valence-bond form. The valence-bond coefficients are found to be real. This transformation was first introduced by Harris and Pohl[22] in their work on the hydrogen halides.

The diatomic Hamiltonian is

$$H(1,2) = -\tfrac{1}{2}\nabla_1^2 - \tfrac{1}{2}\nabla_2^2 + V_1 + V_2 + 1/r_{12} \tag{72}$$

where

$$V_i = -Z_a^c/r_{ia} - Z_b^c/r_{ib} = V_{ia} + V_{ib} \, . \tag{73}$$

The unrestricted MO wave function is

$$\Psi(1,2) = (C_{1a}\,\chi_a + C_{1b}\,\chi_b)(C_{2a}\,\chi_a + C_{2b}\,\chi_b)\,\eta(1,2) \tag{74}$$

where

$$\eta(1,2) = \alpha(1)\beta(2) - \beta(1)\alpha(2) \tag{75}$$

is the spin factor. The equivalent valence-bond wave function is

$$\Psi(1,2) = (b_1\Psi_1 + b_2\psi_2 + b_3\psi_3)\ \eta(1,2) \tag{76}$$

where

$$\psi_1(1,2) = \chi_a(1)\ \chi_a(2) \tag{77}$$

$$\psi_2(1,2) = \chi_b(1)\ \chi_b(2) \tag{78}$$

$$\psi_2(1,2) = \tfrac{1}{2}(\chi_a(1)\ \chi_b(2) + \chi_b(1)\ \chi_a(2)). \tag{79}$$

The numbers 1 and 2 in parenthesis refer to the respective sets of coordinates of the two electrons. The b_i are the coefficients of the valence bond configurations ψ_i.

The electronic energy

$$E = \langle\Psi|H|\Psi\rangle \tag{80}$$

is evaluated in terms of the integrals over atomic orbitals by use of the evaluation procedures described in Chapter II. The energy minimizing set of the b_i is located by determining the value of E systematically at sets (b_1, b_2) in a mesh search procedure; b_3 is determined for each (b_1, b_2) set by requiring that the wave function Ψ be normalized to unity. This procedure was successfully checked against those hydrogen halide results of Harris and Pohl[22] which are displayed in Table IV.

Hydrogen fluoride is used for a test molecule with a 1s SZO for hydrogen and a $2p^{\sigma}$ for fluorine. The ionization potentials, electron

affinities, integrals over atomic orbitals, and $1/R_{HF}$ are varied one at a time by ±10%. The overlap and two-center core integrals and the ionization potential of hydrogen are varied from zero to at least twice the value given by their respective evaluation expressions. The computations are carried out at each of three geometries: one inside (0.688Å), one outside (1.146Å), and one at (0.917Å), the experimental equilibrium internuclear distance[54].

±10% Variations

The effects of ±10 variation of each of several quantities appearing in the electronic energy expression are displayed in Table XXVIII.

It is notable that the effect of variation of a quantity dependent primarily on hydrogen is consistently one to two orders of magnitude less than the effect of variation of the same quantity for fluorine. This seems odd in light of the fact that the ratio of the VSIP's $VSIP_H/VSIP_F$ is about 2/3 and not 1/10 or 1/100. This model characteristic is reflected in the value of the ratio b_1/b_2 of the minimum energy wave function. Thus, the wave function tends toward an ionic form much more rapidly than might to be though from a simple consideration of the ratios of the input quantities determined by each atom. This discrepancy in sensitivity may be a general property of semiempirical methods that rely upon valence electron atomic data or simply a pecularity of the particular model employed.

The change in the sensitivity of the electronic energy with internuclear distance varies strongly from one quantity to another--from changes on the order of electron volts for the one center core integral $H11_{FF}$ to one ten-thousandth of an electron volt for the valence state electron

TABLE XXVIII

CHANGE IN THE ELECTRONIC ENERGY WITH VARIATION OF THE INTEGRALS AND OTHER QUANTITIES Q TO VALUES Q' = K x Q

		Algebraic Change			Percentage Change		
R_{HF}	(Å)	0.688	0.917	1.146	0.688	0.917	1.146
E_R	(e.V.)	-66.50	-56.68	-51.31	-66.50	-56.68	-51.31
Quantity Varied	K	$E - E_R$ (e.V.)			$((E-E_R)/\|E_R\|) \times 100$ (%)		
$VSIP_H$	0.9	-0.014	0.22	0.44	- 0.02	0.40	0.87
	1.1	-0.005	-0.32	-0.59	- 0.01	- 0.56	- 1.15
$VSIP_F$	0.9	2.09	2.06	2.05	3.15	3.64	3.98
	1.1	-2.09	-2.08	-2.07	- 3.15	- 3.66	- 4.02
$VSEA_H$	0.9	0.000	0.001	0.001	0.000	0.002	0.001
	1.1	0.000	-0.001	-0.002	0.000	-0.002	- 0.002
$VSEA_F$	0.9	0.37	0.29	0.22	0.55	0.51	0.43
	1.1	-0.37	-0.30	-0.23	- 0.55	- 0.52	- 0.45
Hl_{HH}	0.9	0.004	0.19	0.49	0.01	0.34	0.95
	1.1	-0.016	-0.45	-0.95	- 0.02	- 0.80	- 1.85
Hl_{FF}	0.9	7.47	5.11	4.15	11.23	9.01	8.09
	1.1	-8.70	-6.73	-5.53	-13.08	-11.87	-10.78
Hl_{HF}	0.9	-0.48	0.62	1.01	- 0.72	1.09	1.96
	1.1	-0.39	-1.18	-1.20	- 0.58	- 2.07	-2.33
(HH|HH)	0.9	-0.001	-0.005	-0.006	- 0.002	- 0.008	-0.012
	1.1	0.001	0.004	0.005	0.002	0.006	-0.010

TABLE XXVIII (Continued)

		Algebraic Change			Percentage Change		
R_{HF}	(Å)	0.688	0.917	1.146	0.688	0.917	1.146
E_R	(e.V.)	-66.50	-56.68	-51.31	-66.50	-56.68	-51.31
Quantity Varied	K	$E - E_R$ (e.V.)			$((E-E_R)/\|E_R\|) \times 100$ (%)		
(FF|FF)	0.9	-1.81	-1.34	-1.01	- 2.72	- 2.37	- 1.98
	1.1	1.69	1.09	0.74	2.53	1.02	1.44
(HH|FF)	0.9	-0.001	-0.14	-0.33	- 0.002	- 0.25	- 0.64
	1.1	0.001	0.10	0.24	0.001	0.17	0.47
(HH|HF)	0.9	0.001	-0.02	-0.03	0.001	- 0.04	- 0.06
	1.1	-0.001	0.02	0.02	- 0.002	0.03	0.05
(FF|FH)	0.9	-0.04	-0.34	-0.35	- 0.06	- 0.60	- 0.67
	1.1	-0.13	0.29	0.34	- 0.20	0.51	0.66
(HF|HF)	0.9	-0.02	-0.02	-0.03	- 0.03	- 0.04	- 0.05
	1.1	0.01	0.02	0.02	0.02	0.04	0.05
ρ_H	0.9	-0.02	0.15	0.19	- 0.02	- 0.27	0.38
	1.1	-0.01	-0.17	-0.20	- 0.01	- 0.29	- 0.39
ρ_F	0.9	-0.03	0.19	0.25	- 0.04	0.34	0.49
	1.1	-0.01	-0.22	-0.26	- 0.02	- 0.39	- 0.50
$1/R_{HF}$	0.9	4.10	2.56	1.81	6.17	4.51	3.53
	1.1	-4.29	-2.77	-1.96	- 6.45	- 4.89	- 3.82
S_{HF}	0.9	0.004	0.11	0.20	0.01	0.19	0.39
	1.1	-0.005	-0.11	-0.20	- 0.01	- 0.20	- 0.39

affinity of hydrogen.

Variation of the Overlap Integral

For some time it has been common practice for chemists to attempt qualitative assessments of transition-state stabilities based solely upon considerations of the orbital overlap. A recent example of such an attempt has been given by Gimarc[72], who employed orbital overlap considerations in a Hückel model to deduce a plausible mechanism for the (H_2,D_2) exchange reaction. Because of the frequent usage of such procedures, especially in organic chemistry, and because of the key role of the overlap integral in semiempirical molecular models, special consideration is given to the determination of the model sensitivity to the value assigned to the orbital overlap S_{AB}.

Table XXIX and Figures 12 and 13 illustrate the calculated electronic energy variation at each of the three intercore separations given above for a wide-range variation of S_{AB} ($S'_{AB} = K \times S_{AB}$, $0 \leq K \leq 2$). As expected, the electronic energy decreases ($|E|$ increases) with increase of S_{AB} at each of the three geometries R_{HF} = 0.688, 0.917, and 1.146Å, but the sensitivity to S_{AB} increases sharply as the intercore distance increases. It should be noted that intercore distances in excess of the equilibrium spacing are usually involved whenever one considers the transition-state in a chemical reaction. The present computations clearly indicate that for such geometries one may expect a pronounced dependence of stability upon overlap. If this dependence is not an artifact of the semiempirical formulation being employed and is reflected in an accurate full configuration interaction ab initio calculation, then assessment of transition-state stability based solely upon overlap con-

TABLE XXIX

CHANGE IN THE ELECTRONIC ENERGY WITH VARIATION OF THE OVERLAP INTEGRAL S TO VALUES S' = K x S

	Algebraic Change			Percentage Change		
R_{HF} (Å)	0.688	0.917	1.146	0.688	0.917	1.146
E_R (e.V.)	-66.50	-56.68	-51.31	-66.50	-56.68	-51.31
S_{HF}	0.3355	0.2989	0.2410	0.3355	0.2989	0.2410
K		$E - E_R$ (e.V.)			$((E-E_R)/\|E_R\|) \times 100$ (%)	
0.0	0.622	0.64	1.55	0.935	1.13	3.02
0.1	0.011	0.63	1.52	0.017	1.12	2.97
0.2	0.011	0.61	1.44	0.017	1.08	2.81
0.3	0.011	0.57	1.32	0.016	1.01	2.57
0.4	0.011	0.52	1.16	0.016	0.92	2.27
0.5	0.010	0.46	0.99	0.015	0.81	1.92
0.6	0.009	0.39	0.80	0.014	0.68	1.56
0.7	0.008	0.30	0.60	0.012	0.53	1.18
0.8	0.006	0.21	0.40	0.009	0.37	0.79
0.9	0.004	0.11	0.20	0.005	0.19	0.39
1.0	0.000	0.00	0.00	0.000	0.00	0.00
1.1	-0.005	-0.11	-0.20	-0.007	-0.20	-0.39
1.2	-0.012	-0.23	-0.40	-0.017	-0.40	-0.77
1.3	-0.020	-0.35	-0.59	-0.030	-0.61	-1.15
1.4	-0.031	-0.47	-0.78	-0.047	-0.82	-1.53
1.5	-0.045	-0.59	-0.97	-0.068	-1.03	-1.89
1.6	-0.064	-0.71	-1.16	-0.096	-1.25	-2.25
1.7	-0.087	-0.83	-1.34	-0.130	-1.46	-2.60
1.8	-0.116	-0.95	-1.51	-0.174	-1.68	-2.95
1.9	-0.153	-1.07	-1.68	-0.230	-1.89	-3.28
2.0	-0.200	-1.19	-1.85	-0.301	-2.10	-3.61

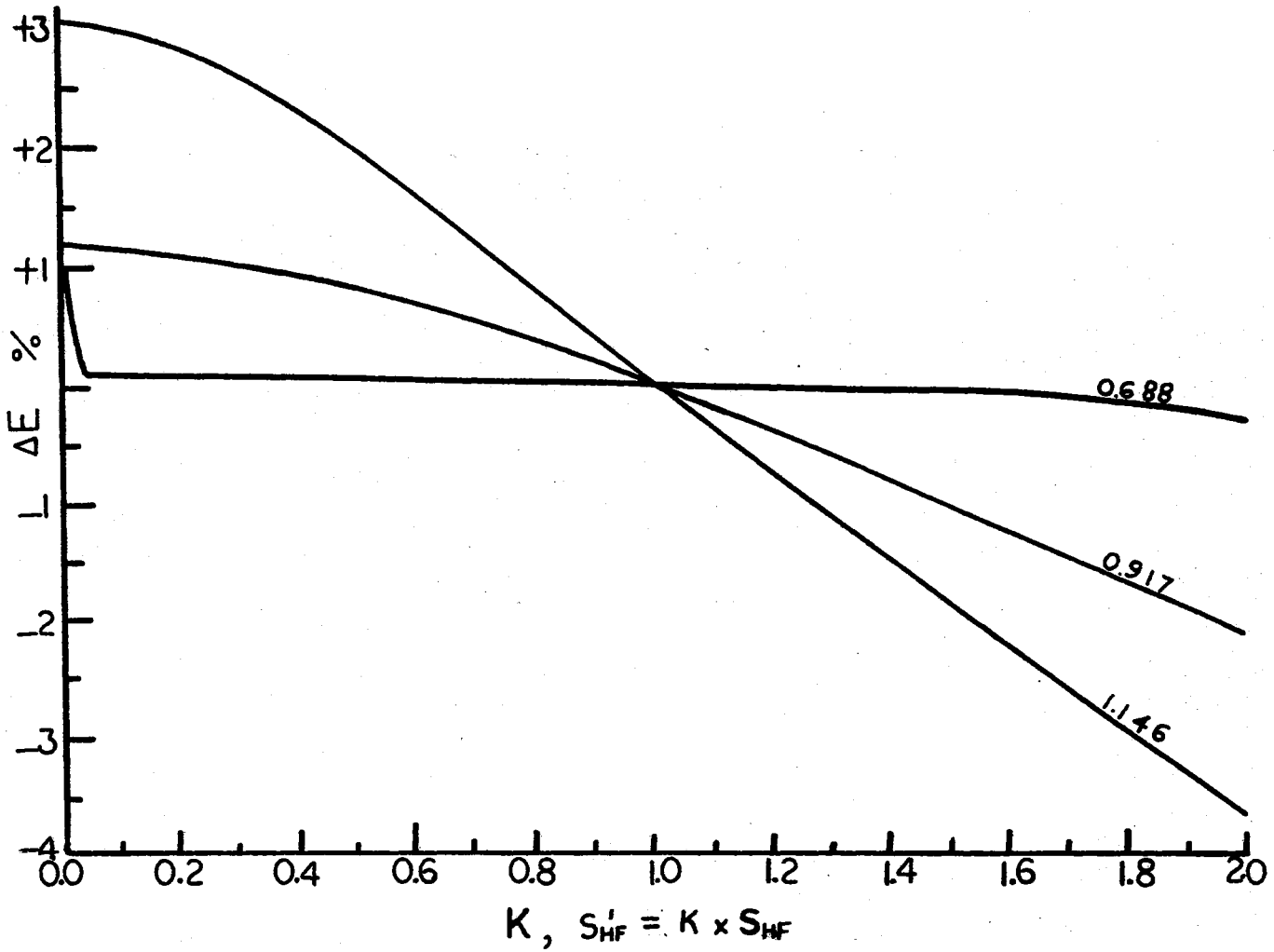

Figure 12. Percentage Change in E vs. Variation of S_{HF} at R_{HF} = 0.688, 0.917, and 1.146 Angstroms

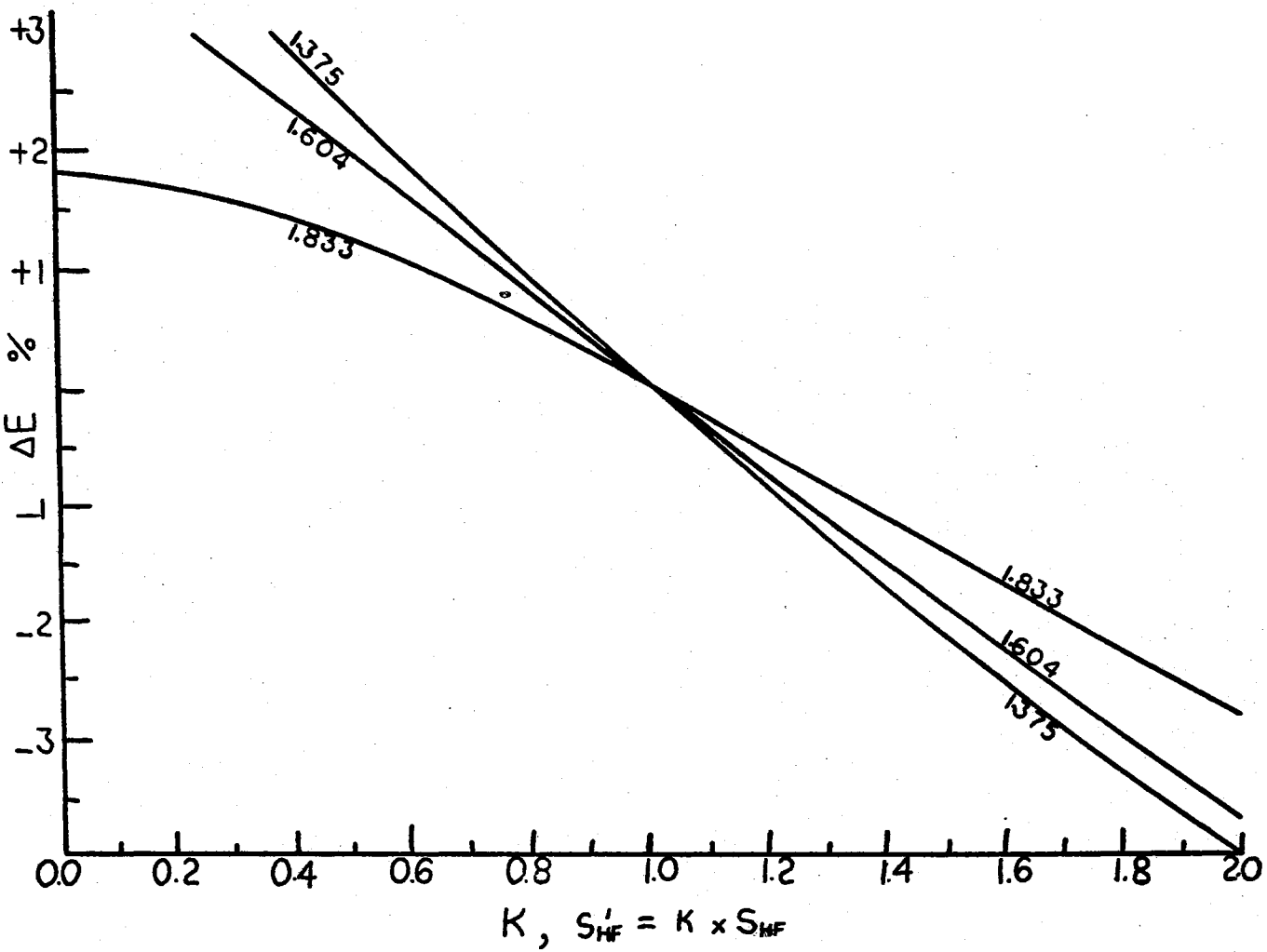

Figure 13. Percentage Change in E vs. Variation of S_{HF} at R_{HF} = 1.375, 1.604, and 1.833 Angstroms

siderations would be a reasonable procedure which would likely yield qualitatively correct results and viable mechanisms. On the other hand, if such a pronounced dependence is not reflected in the full computations, then erroneous conclusions regarding the stability of transition-state complexes and incorrect mechanisms may result.

Variation of the Wolfsberg-Holmholz-like Parameter

The sensitivity of the model to a Wolfsberg-Holmholz[19] type of parameter may be determined by varying the two-center one-electron integral $H12_{ab}$, symbolized by $H1_{HF}$ in the illustrations. The results of such a variation are shown in Table XXX and Figure 14. As can be seen, for each geometry there exists a maximum in the electronic energy in the range $0.8 \leq K \leq 1.0$, where $H1_{HF}' = K \times H1_{HF}$. On either side of these maxima the electronic energy decreases in a nearly linear fashion, and the wave function becomes increasingly covalent (i.e. the magnitude of b_3 increases). Sensitivity to the parameter is about the same at all three geometries.

While it may appear that the Wolfsberg-Holmholz-like parameter K could be varied up or down to decrease the electronic energy a given amount, it turns out that b_3 becomes negative and the molecular orbitals computed from the valence bond coefficients become antisymmetric for K appreciably less than 1. This phenomenon for $K < 1$ has been used by Cusachs[73] to place a lower bound to the integral $H12_{ab}$.

Variation of a Sample Ionization Potential

Wide range variation of the valence state ionization potential of hydrogen gives largely the expected qualitative results (Table XXXI and

TABLE XXX

CHANGE IN THE ELECTRONIC ENERGY WITH VARIATION OF THE INTEGRAL $H1_{HF}$ TO VALUES $H1_{HF}' = K \times H1_{HF}$

	Algebraic Change			Percentage Change		
R_{HF} (Å)	0.688	0.917	1.146	0.688	0.917	1.146
E_R (e.V.)	-66.50	-56.68	-51.31	-66.50	-56.68	-51.31
$H1_{HF}$ (e.V.)	-14.56	-12.19	- 9.45	-14.56	-12.19	- 9.45
K		$E - E_R$ (e.V.)			$((E-E_R)/\|E_R\|) \times 100$ (%)	
0.0	-22.68	-13.64	- 5.71	-34.11	-24.07	-11.13
0.2	-16.68	-10.00	- 4.25	-25.08	-17.65	- 8.29
0.4	-11.60	- 6.37	- 2.11	-17.45	-11.23	- 4.10
0.5	- 8.82	- 4.55	- 1.03	-13.27	- 8.02	- 2.01
0.6	- 6.28	- 2.73	0.04	- 9.45	- 4.81	- 0.08
0.7	- 3.64	- 0.75	0.99	- 5.48	- 1.32	1.93
0.75	------	- 0.31	1.41	------	- 0.55	2.74
0.8	- 1.85	0.29	1.55	- 2.79	0.51	3.01
0.85	------	0.59	1.37	------	1.05	2.67
0.9	- 0.48	0.62	1.01	- 0.72	1.09	1.96
0.95	- 0.13	0.40	0.54	- 0.19	0.71	1.05
1.0	0.00	0.00	0.00	0.00	0.00	0.00
1.05	- 0.09	- 0.54	- 0.58	- 0.14	- 0.95	- 1.13
1.1	- 0.39	- 1.18	- 1.20	- 0.58	- 2.07	- 2.33
1.2	- 1.47	- 2.64	- 2.49	- 2.21	- 4.65	- 4.85
1.3	- 2.99	- 4.25	- 3.85	- 4.50	- 7.49	- 7.49
1.4	- 4.76	- 5.94	- 5.24	- 7.15	-10.48	-10.21
1.6	- 8.65	- 9.46	- 8.10	-13.01	-16.70	-15.79
1.8	-12.76	-13.08	-11.62	-19.19	-23.07	-21.48
2.0	-16.97	-16.74	-13.98	-25.51	-29.53	-27.25
5.0	------	-72.72	------	------	-128.3	------

TABLE XXXI

CHANGE IN THE ELECTRONIC ENERGY WITH VARIATION

OF $VSIP_H$ TO VALUES $VSIP_H' = K \times VSIP_H$

	Algebraic Change			Percentage Change		
R_{HF} (Å)	0.688	0.917	1.146	0.688	0.917	1.146
E_R (e.V.)	-66.50	-56.68	-51.31	-66.50	-56.68	-51.31
K		$E - E_R$ (e.V.)			$((E-E_R)/\|E_R\|) \times 100$ (%)	
0.0	- 0.50	0.60	1.54	- 0.75	1.06	3.00
0.5	- 0.18	0.60	1.30	- 0.27	1.06	2.53
0.6	- 0.13	0.56	1.18	- 0.19	0.98	2.29
0.7	- 0.08	0.49	1.01	- 0.12	0.86	1.96
0.8	- 0.04	0.38	0.77	- 0.07	0.67	1.50
0.9	- 0.01	0.22	0.44	- 0.02	0.40	0.87
1.0	0.00	0.00	0.00	0.00	0.00	0.00
1.1	- 0.01	- 0.32	- 0.59	- 0.01	- 0.56	- 1.15
1.2	- 0.04	- 0.76	- 1.33	- 0.06	- 1.34	- 2.60
1.3	- 0.12	- 1.35	- 2.22	- 0.18	- 2.38	- 4.33
1.4	- 0.27	- 2.10	- 3.23	- 0.41	- 3.71	- 6.30
1.5	- 0.55	- 3.00	- 4.34	- 0.83	- 5.29	- 8.45
2.0	- 5.07	- 8.80	-10.6	- 7.62	-15.5	-20.6
5.0	-49.0	-49.7	-51.3	-69.2	-87.7	-100.

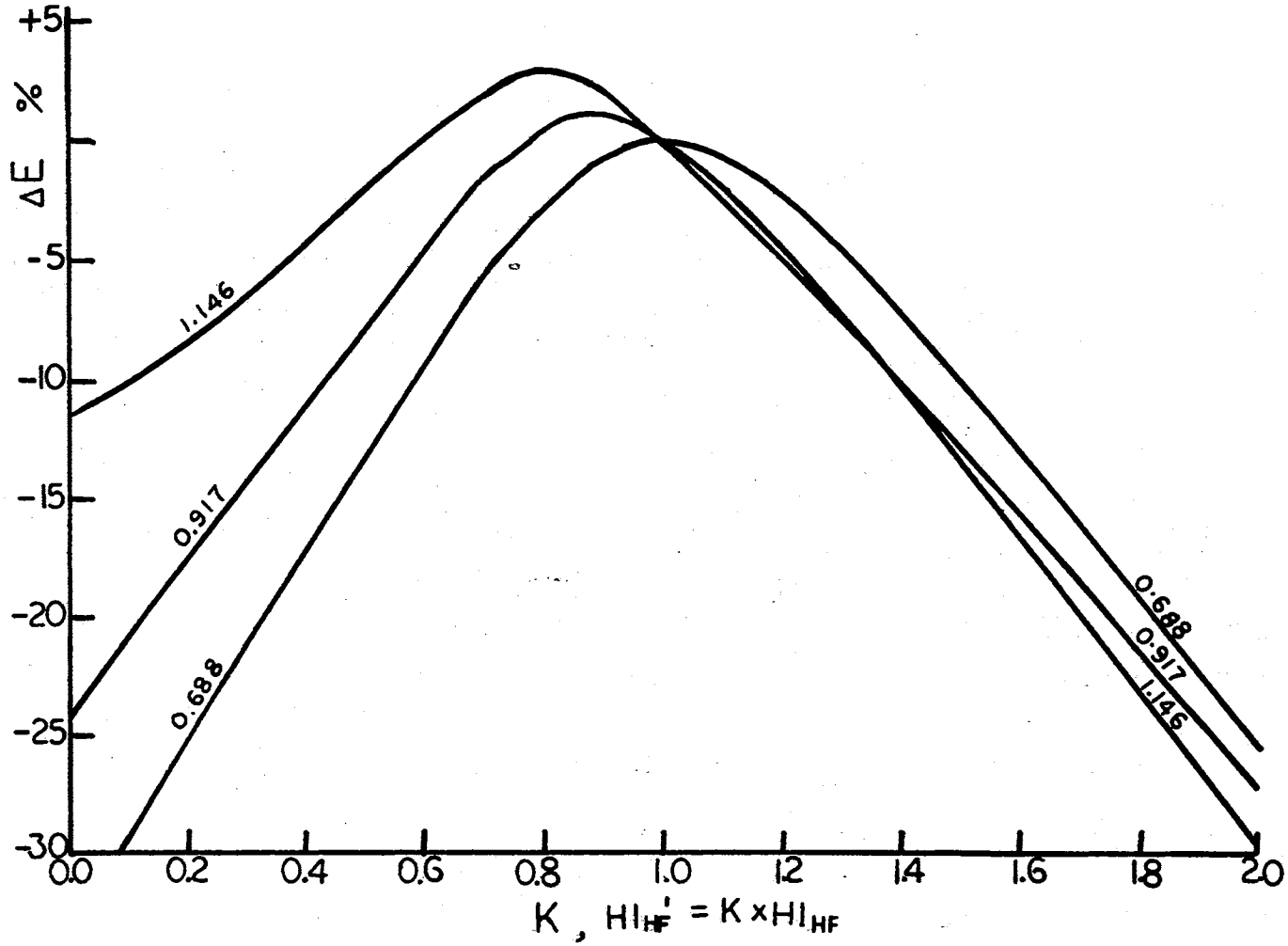

Figure 14. Percentage Change in E vs. Variation of HI_{HF} at R_{HF} = 0.688, 0.917, and 1.146 Angstroms

Figure 15). The electronic energy decreases monotonically at the two largest values of the intercore distance as the valence state ionization potential is varied from zero to twice its value ($VSIP_H' = K \times VSIP_H$, $0 \leq K \leq 2$). At the smallest distance, E decreases monotonically as the ionization potential is varied up or down form its value. Meanwhile, the sensitivity increases with the intercore distance; the wave function varies from ionic (H^+F^-) through covalency to ionic ($H^{-f}F^{+f}$) as K is varied from 0 to 5. At K = 5, f(0.688) = 0.5, f(0.917) = 0.2, and f(1.146) = 0.1. The decrease of f with R_{HF} indicates that a distance dependent expression for the valence state ionization potential may be useful in semiempirical molecular models. That f approaches 1 only at small R_{HF} is due the fact ρ_F is about 25% larger in magnitude than ρ_H.

Discussion

The forms and magnitudes of variation found may be used as guidance in determining the relative merits of alternative integral evaluation and approximation expressions. Computations of the particular integral concerned by the reference and trial forms of the integral approximation expressions yields information on their relative merit in matching the experimental results. For example, choice of a tetrahedral orbital to represent fluorine in the computation of the overlap S_{HF} using the same experimental quantities and orbital parameters as used for the $2p^\sigma$ orbital gives larger overlaps (see Table XXXII) and, therefore, reduced electronic energies (increased $|E|$), but the effect is greater as the intercore distance R_{HF} increases from 0.688 to 1.146Å (see Table XXVIII, Table XXIX, or Figure 15). Beyond R = 1.146Å, the decreasing magnitude of S_{HF} reduces its quantitative effect on the electronic energy (see

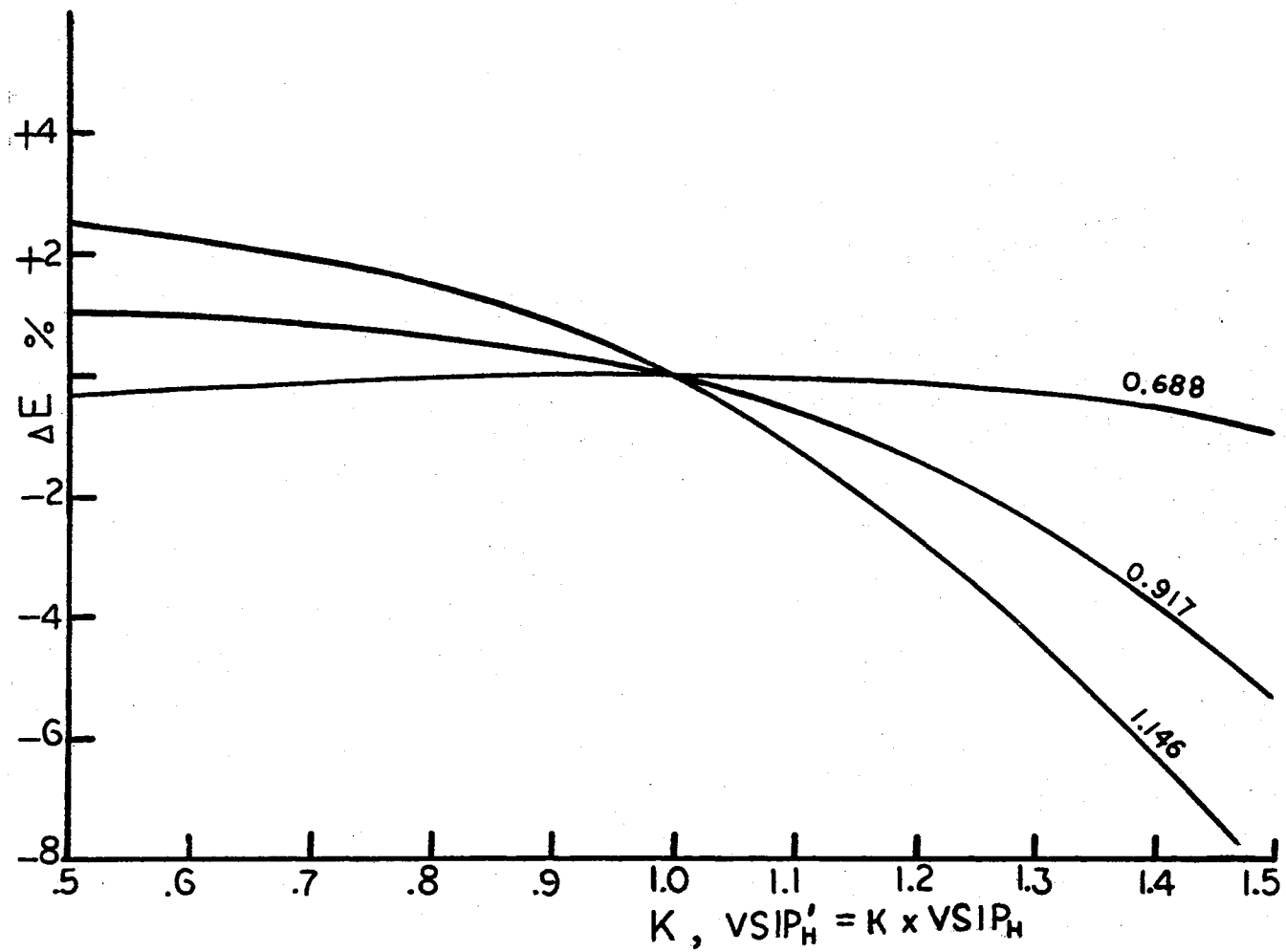

Figure 15. Percentage Change in E vs. Variation of $VSIP_H$ at R_{HF} = 0.688, 0.917, and 1.146 Angstroms

Figure 13). Thus, use of the tetrahedral orbital for fluorine is expected to increase the amount of covalency and, for a given core repulsion energy approximation expression, increase both the magnitude of the computed equilibrium intercore distance and the magnitude of the molecular binding energy. These expectations are born out by comparative computations for HF with fluorine characterized by a $2p^{\sigma}$ and a $2te^{\sigma}$ orbital; the results are displayed in Table XXXII and Figure 16. Exact matching fits of the polynomial expression.

$$E_{BIND} = \sum_{i=o}^{5} a_i R^i \tag{81}$$

to the tabulated binding energies in Table XXXII give the calculated equilibrium distances, binding energies, and force constants as 0.909 $\mathring{A}$, -5.52 e.V., and 14.8 x 10^5 dynes/cm for $2p^{\sigma}$ fluorine and as 0.937 $\mathring{A}$, -6.31 e.V., and 12.9 x 10^5 dynes/cm for $2te^{\sigma}$ fluorine compared with 0.9171 $\mathring{A}$, -6.40 e.V., 8.8 x 10^5 dynes/cm from experiment[57].

While the variations observed in this paper apply to the Harris-Pohl semiempirical molecular model in particular, it is expected that the results to be of value in determining the set of parameters and integral approximation expressions which will optimize selected valence electron models.

TABLE XXXII

COMPARISON OF THE USE OF A $2p^{\sigma}$ WITH A $2te^{\sigma}$ VALENCE ORBITAL TO DESCRIBE FLUORINE FOR OVERLAP COMPUTATION

R_{HF} (Å)	S_{HF}		E		E_{CR} †	E_{BIND}#	
	$1s\text{-}2p^{\sigma}$	$1s\text{-}2te^{\sigma}$	$2p^{\sigma}$	$2te^{\sigma}$		$2p^{\sigma}$	$2te^{\sigma}$
			(e.V.)		(e.V.)	(e.V.)	
0.688	0.3355	0.5973	-66.50	-66.61	30.28	-1.64	-1.75
0.917	0.2989	0.4946	-56.68	-57.45	16.57	-5.52	-6.29
1.146	0.2410	0.3825	-51.31	-52.44	12.56	-4.16	-5.29
1.375	0.1823	0.2823	-47.71	-48.81	10.47	-2.66	-3.76
1.604	0.1325	0.2017	-45.11	-46.00	8.98	-1.54	-2.44
1.833	0.0936	0.1408	-43.23	-43.85	7.86	-0.79	-1.41

† $E_{CR} = 1/R_{HF} + E_{CORR}$. E_{CORR} and the procedure for getting it from the Herman-Skillman[46] potential for fluorine is as given by Pohl, Rein, and Appel[21] and tabulated by Harris and Pohl[22].

$E_{BIND} = E + E_{CR} - E_H - E_F$, where $E_A = -VSIP_A$.

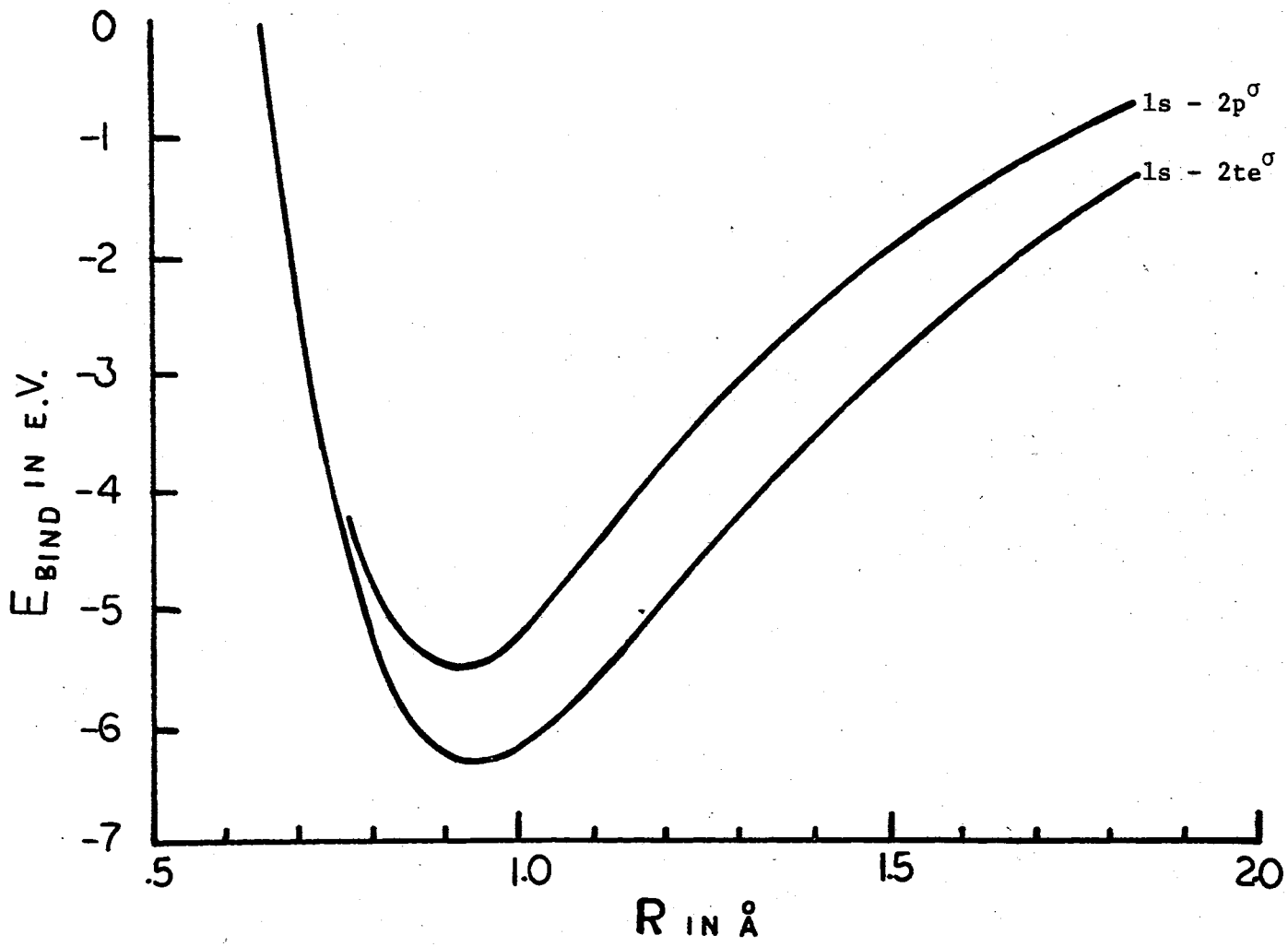

Figure 16. E_b vs. R_{HF} for Fluorine Hybridizations $2p^{\sigma}$ and $2te^{\sigma}$

CHAPTER VI

CONCLUSION

Summary

The selected valence electron model developed in this study is capable of describing several molecular properties. Computed bond lengths are often within experimental error of the correct values. Bond energies and stretching frequencies can be properly sequenced through several homologous series of halogen compounds: the hydrogen halides, haloethenes, haloethynes and halobenzenes. Equilibrium bond angles are accurately computed from a consideration of only the bonding electron pairs along the angle-forming bonds. The model is also capable of a proper qualitative treatment of the molecular dipole moments and ionization potentials through the mono-halogen series. For the isomers of dichloroethene, bond length predictions and are good as is the qualitative account of the dipole moment variation.

Overall, it is concluded from this study that semiempirical molecular models which consider only information on some of the valence electrons have the flexibility to properly determine many molecular characteristics. Calibration will be required to obtain quantitative results for several computed properties at once. In particular, the core repulsion expression parameters must be carefully chosen to achieve the correct ordering of the bond energies through a series or to enable the model to account for H-H and C-H bonds. The concept of bond character-

istic parameters must be adopted and optimum values determined.

Plans for Further Work

Effort may now be allocated to the problem of choosing, for a given selected valence electron model, an optimum combination of (1) experimental atomic data, (2) atomic orbitals, (3) integral approximations, and (4) core repulsion expression. Preliminary steps in this direction are described in Chapter V. The goal of this project will be to develop the capability to determine, in advance, the best set of the components (1)-(4) once a particular model is conceived. With this capability, several selected electron models could be examined easily for a class of molecules and their relative information content compared.

Once the choice of components is made, further optimization--fine tuning--may be realized by a proper placement and choice of valves for adjustable parameters. The positioning of parameters in the core repulsion expression and the two-center one-electron core integral have been discussed in this study. It will be noticed that in both cases the parameter placement is as to avoid bias to one or the other of two atoms. The use of atom-pair characteristic parameters is not new[9-12,15-17]. However, it is proposed here that the parameters be taken to be bond-pair rather than atom-pair dependent. It is specifically proposed that model flexibility which allows the description of an atom in different bonding situations be required. Carbon, in particular, must be accounted for in single, double and triple bonds. One way would be to introduce separate pi and sigma parameters; another, one parameter per atom per distinct bond type.

Considering the success of the limited information input model of

this study, but recognizing its dependency upon known molecular geometries, the following proposal is made: an effort should be made to develop a one electron per atom molecular model in which each atom is characterized in the atomic orbital basis set by one especially chosen function. These one electron-one atom functions are to be formulated in such a way as to allow the model to account for all of the geometric specifications of the molecule--i.e., bond lengths, three center angles, dihedral angles. One such function would be an equal weighted and normalized linear combination of s, q_x, q_y, and q_z AO's, where q_i represents an AO equivalent to a pi AO except that it is positive throughout all space. A successful demonstration of such a model would be a step in the development of a new concept in approximate wave functional forms for use in the description of molecular properties by semiempirical quantum methods.

SELECTED BIBLIOGRAPHY

1. Pilar, F. L. Elementary Quantum Chemistry. New York: McGraw-Hill Book Company, 1968.

2. Dirac, P. A. M. Quoted in Levine, Ira N. Quantum Chemistry, Volume I: Quantum Mechanics and Molecular Electronic Structure. Boston: Allyn and Bacon, 1970, 562.

3. Mulliken, R. S. and Roothaan, C. C. J. Proc. Natl. Acad. Sci. U.S., 45, 394 (1959).

4. Clementi, E. J. Chem. Phys., 46, 3851 (1967).

5. Clementi, E. J. Chem. Phys., 47, 2323 (1967).

6. Pariser, R. and Parr, R. G. J. Chem. Phys., 21, 466, 767 (1953).

7. Pople, J. A. Trans. Faraday Soc., 49, 1375 (1953).

8. Hoffman, R. J. Chem. Phys., 39, 1397 (1963).

9. Pople, J. A., Santry, D. P., and Segal, G. A. J. Chem. Phys., 43, S129 (1965).

10. Pople, J. A. and Segal, G. A. J. Chem. Phys., 43, S136 (1965).

11. Pople, J. A. and Segal, G. A. J. Chem. Phys., 44, 3289 (1965).

12. Pople, J. A., Beveridge, D. L., and Dobosh, P. A., J. Chem. Phys., 47, 2026 (1967).

13. Klopman, G. J. Amer. Chem. Soc., 86, 1463, 4550 (1964), 87, 3300 (1965). The abbreviation "KINDO" for Klopman's INDO-like method is here introduced.

14. Dixon, R. N. Mol. Phys., 12, 83 (1967).

15. Dewar, M. J. S. and Klopman, G. J. Amer. Chem. Soc., 89, 3089 (1967).

16. Baird, N. C. and Dewar, M. J. S. J. Chem. Phys., 50, 1262 (1969).

17. Dewar, M. J. S. and Haselbach, E. J. Amer. Chem. Soc., 92, 590 (1970).

18. Fischer-Hjalmers, I. Arkiv Fysik, 21, 123 (1962).

19. Wolfsberg, M. and Helmholz, L. J. Chem. Phys., 20, 837 (1952), 838.

20. Bodor, N., Dewar, M. J. S., Harget, A., and Haselbach, E. J. Amer. Chem. Soc., 92, 3854 (1970).

21. Pohl, H. A., Rein, R., and Appel, K. J. Chem. Phys., 41, 3385 (1964).

22. Harris, F. E. and Pohl, H. A. J. Chem. Phys., 42, 3648 (1965).

23. Pohl, H. A. and Raff., L. M. Int. J. Quan. Chem., I, 577 (1967).

24. Mickish, D. J. and Pohl, H. A. "Simplified SCF Calculations for Sigma-Bonded Systems: Extension to Hydrogen Bonding." Sigma Molecular Orbital Theory. Ed. Oktay Sinanoğlu and Kenneth B. Wiberg. New Haven: Yale University Press, 1970, 105-114.

25. Cantril, J. M. and Pohl, H. A. Int. J. Quan. Chem., IV, 165 (1971).

26. Rein, R. and Harris, F. E. J. Chem. Phys., 41, 3393 (1964).

27. Raff, L. M., Stivers, L., Porter, R. N., Thompson, D. L., and Sims, L. B. J. Chem. Phys., 52, 3449 (1970).

28. London, F. Z. Electrochem., 35, 552 (1929).

29. Slater, J. C. Phys. Rev., 38, 1109 (1931). Proof of London's four center equation of Ref. 28.

30. Eyring, H. and Polanyi, M. Z. Physik. Chem. (Leipzig), B12, 279 (1931).

31. Sato, S. J. Chem. Phys., 23, 592, 2465 (1955).

32. Cashion, J. K. and Herschback, D. R. J. Chem. Phys., 40, 2358 (1964).

33. Sullivan, J. H. J. Chem. Phys., 39, 3001 (1963).

34. Slater, J. C. Phys. Rev., 36, 57 (1930).

35. Zener, C. Phys. Rev., 36, 51 (1930).

36. Mulliken, R. S., Rieke, C. A., Orloff, D., and Orloff, H. J. Chem. Phys., 17, 1248 (1949).

37. Goepport-Mayer, M. and Sklar, A. L. J. Chem. Phys., 6, 645 (1938), Eq. 37.

38. Mulliken, R. S. J. Chim. Phys., 46, 497 (1949), in the English summary on page 500.

39. Pariser, R. J. Chem. Phys., 21, 568 (1953).

40. Hinze, J. and Jaffe', H. H. J. Amer. Chem. Soc., 84, 540 (1962); J. Phys. Chem., 67, 1501.

41. Pritchard, H. O. and Skinner, H. A. Chem. Rev., 55, 745 (1955).

42. Roothaan, C. C. J. Rev. Mod. Phys., 23, 69 (1951).

43. Pople, J. A. and Nesbet, R. K. J. Chem. Phys., 22, 571 (1954).

44. Hall, G. G. Matrices and Tensors. The International Encyclopedia of Physical Chemistry and Chemical Physics, Topic 1, IV. Ed. H. Jones. New York: Pergamon Press, 1963.

45. Mulliken, R. S. J. Chem. Phys., 23, 1833, 1841, 2338, 2343 (1955); 36, 3428 (1962).

46. Herman, F. and Skillman, S. Atomic Structure Calculations. Englewood Cliffs: Prentice-Hall, Inc., 1963.

47. Private communication.

48. Dewar, M. J. S. The Molecular Orbital Theory of Organic Chemistry. New York: McGraw-Hill Book Company, 1969, 463ff.

49. Davies, D. W. The Theory of the Electric and Magnetic Properties of Molecules. New York: John Wiley and Sons, 1967, 76-83.

50. Rosser, J. B., Lanczos, C., Hestenes, M. R., and Karush, W. J. Res. Nat. Bur. Stds., 47, 291-297 (1951).

51. Gregory, R. T. and Karney, D. L. A Collection of Matrices for Testing Computational Algorithms. New York: Wiley-Interscience, 1969, 61-2.

52. Pople, J. A., Gordon, M. J. Amer. Chem. Soc., 89, 4253 (1967).

53. Baird, N. C., Dewar, M. J. S. Theoret. Chim. Acta (Berl.), 9, 1 (1967).

54. Cottrell, T. L. The Strength of Chemical Bonds. New York: Academic Press, Inc., 1954.

55. Weast, R. C. (Ed.). Handbook of Chemistry and Physics, 45th ed. Cleveland: The Chemical Rubber Co., 1964, E41.

56. Yukawa, Y. (Ed.). Handbook of Organic Structural Analysis, New York: W. A. Benjamin, Inc., 1965.

57. Keller, R. Basic Tables in Chemistry. New York: McGraw-Hill Book Company, 1967.

58. Herzberg, G. Molecular Spectra and Molecular Structure. II. Infrared and Raman Spectra of Polyatomic Molecules. Princeton: D. Van Nostrand Company, Inc., 1945, 9th printing, 195.

59. McClellan, A. L. Tables of Experimental Dipole Moments. San Francisco: W. H. Freeman and Company, 1963.

60. Vedeneyev, V. I., Gurvich, L. V., Konrat' yev, V. N., Medvedeu, V. A., and Frankevich, ye.L. Bond Energies, Ionization Potentials, and Electron Affinities. New York: St. Martin's Press, 1966.

61. Sheppard, W. A. and Sharts, C. M. Organic Fluorine Chemistry. New York: W. A. Benjamin, Inc., 1969.

62. Hunt, G. R. and Wilson, M. K. J. Chem. Phys., 34, 1301 (1961).

63. Hediger, H. J. Infrared Structural Correlation Tables. Eds. R. G. J. Miller and H. A. Willis. London: Heydon and Sons Limited, 1964.

64. Bloor, J. E. and Breen, D. L. J. Phys. Chem., 72, 716 (1968).

65. Knowlton, P. and Carper, W. R. Mol. Phys., 11, 213 (1966).

66. Wilson, Jr., E. B., Decius, J. C., Cross, P. C. Molecular Vibrations. The Theory of Infrared and Raman Vibrational Spectra: New York; McGraw-Hill Book Company, Inc., 1955.

67. Allen, L. C. Sigma Molecular Orbital Theory. Eds. O. Sinanoğlu and K. B. Wiberg. New Haven: Yale University Press, 1970, 233.

68. See Ref. 27. For more detail, see Stivers, L. E. Master's Thesis, Oklahoma State University, 1968.

69. Minn, F. L. and Hanratty, A. B. J. Chem. Phys., 53, 2543 (1970).

70. Mataga, N. and Nishimoto, K. J. Chem. Phys., 13, 140 (1954).

71. Pople, J. A. and Gordon, M. J. Amer. Chem. Soc., 89, 4253 (1967).

72. Gimarc, B. M. J. Chem. Phys., 53, 1623 (1970).

73. Cusachs, L. C. Int. J. Quan. Chem., IS, 419 (1967).

74. Handbook of Physics. Eds. E. U. Condon and H. Odishaw, New York: McGraw-Hill Book Company, Inc., 1958, 7-105.

APPENDIX

CONSTANTS AND UNIT CONVERSION FACTORS

The physical constants and dependent unit conversion factors used in this thesis are those given by the 1963 convention[74]. The physical constants are

$$1 \text{ atomic mass unit} = 1.66024 \times 10^{-24} \text{ g.}$$

and

$$1 \text{ electron charge} = -1.60210 \times 10^{-19} \text{ coulomb.}$$

The unit conversion factors are

$$1 \text{ coulomb-meter} = 0.3 \times 10^{30} \text{ Debyes,}$$

$$1 \text{ esu-angstrom} = 4.80630 \text{ Debyes,}$$

$$1 \text{ e.V./particle} = 23.061 \text{ Kcal/mole,}$$

$$1 \text{ a.u. (length)} = 0.529167 \text{ Angstroms,}$$

$$1 \text{ a.u. (energy)} = 27.2107 \text{ e.V.,}$$

and

$$1 \text{ a.u.(energy)}\text{——}\text{a.u.(length)} = 14.399 \text{ e.V.}\text{——}\text{Å.}$$

where esu = electrostatic unit and a.u. = atomic unit.

VITA ≥

Darrel Gene Hopper

Candidate for the Degree of

Doctor of Philosophy

Thesis: SELECTED VALENCE ELECTRON MODEL FOR HALOGEN-SUBSTITUTED PLANAR PI-MOIETY MOLECULES AND SMALL SIGMA-BONDED SYSTEMS

Major Field: Chemistry

Biographical:

Personal Data: Born in Stillwater, Oklahoma, June 10, 1944, the son of Doyle and Dorthea Hopper.

Education: Graduated from Plainview High School, Plainview, Texas, in May, 1962; received the Bachelor of Science degree in chemistry from Oklahoma State University in May, 1966, graduating 2/716 in the College of Arts and Sciences; completed requirements for the Doctor of Philosophy degree at Oklahoma State University in July, 1971.

Professional Experience: National Science Foundation Undergraduate Research Participant, Summers of 1964 and 1965; Engineer, General Electric Company, Summer 1966; Graduate Teaching Assistant, Oklahoma State University, 1966-1969, 1970.